

UNIVERSIDADE DE SÃO PAULO
ESCOLA POLITÉCNICA
DEPARTAMENTO DE ENGENHARIA DE MINAS E DE PETRÓLEO

PAULO HENRIQUE RANAZZI

Analysis of Main Parameters in Adaptive ES-MDA History Matching

Santos
2019

PAULO HENRIQUE RANAZZI

Analysis of Main Parameters in Adaptive ES-MDA History Matching

Dissertation presented to the Graduate Program in Mineral Engineering at the Polytechnic School, University of Sao Paulo to obtain the degree of Master of Science.

Concentration Area: Mineral Engineering

Advisor: Marcio Augusto Sampaio Pinto, PhD

Santos

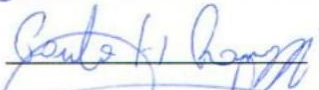
2019

Autorizo a reprodução e divulgação total ou parcial deste trabalho, por qualquer meio convencional ou eletrônico, para fins de estudo e pesquisa, desde que citada a fonte.

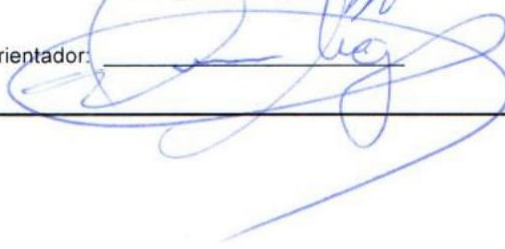
Este exemplar foi revisado e corrigido em relação à versão original, sob responsabilidade única do autor e com a anuência de seu orientador.

São Paulo, 05 de julho de 2019

Assinatura do autor:



Assinatura do orientador:



Catálogo-na-publicação

Ranazzi, Paulo Henrique

Analysis of Main Parameters in Adaptive ES-MDA History Matching / P.
H. Ranazzi -- versão corr. -- São Paulo, 2019.

81 p.

Dissertação (Mestrado) - Escola Politécnica da Universidade de São Paulo. Departamento de Engenharia de Minas e Petróleo.

1. History Matching 2. Ensemble Smoother 3. Localization 4. Uncertainty Assessment I. Universidade de São Paulo. Escola Politécnica. Departamento de Engenharia de Minas e Petróleo II.t.

ACKNOWLEDGEMENTS

Foremost, I would like to thank my family and friends for the constant support.

I would like to express my sincere gratitude to my advisor Prof. Marcio Sampaio for the continuous support of my master's study and research, for motivating me, and for sharing all his knowledge.

Thanks to the Coordination for Improvement of Higher Education Personnel (CAPES) that has provided the financial support during the research.

I am grateful to UNISIM group for providing the simulation model of the benchmark UNISIM-I-H and Computer Modelling Group (CMG) for providing the basic licenses of the flow simulator used in this study.

Last but not the least, I would like to thank Polytechnic School of the University of São Paulo (USP) and Laboratory of Petroleum Reservoir Simulation and Management (LASG) for providing the required infrastructure to perform the research.

*“Explore the world. Nearly everything is really
interesting if you go into it deeply enough.”
(Richard P. Feynman)*

ABSTRACT

RANAZZI, Paulo Henrique. **Analysis of Main Parameters in Adaptive ES-MDA History Matching**. 2019. 81 p. Dissertation (Master's in science) – Polytechnic School, University of São Paulo, Santos, 2019.

In reservoir engineering, history matching is the technique that reviews the uncertain parameters of a reservoir simulation model in order to obtain a response according to the observed production data. Reservoir properties have uncertainties due to their indirect acquisition methods, that results in discrepancies between observed data and reservoir simulator response. A history matching method is the Ensemble Smoother with Multiple Data assimilation (ES-MDA), where an ensemble of models is used to quantify the parameters uncertainties. In ES-MDA, the number of iterations must be defined previously the application by the user, being a determinant parameter for a good quality matching. One way to handle this, is by implementing adaptive methodologies when the algorithm keeps iterating until it reaches good matchings. Also, in large-scale reservoir models it is necessary to apply the localization technique, in order to mitigate spurious correlations and high uncertainty reduction of posterior models. The main objective of this dissertation is to evaluate two main parameters of history matching when using an adaptive ES-MDA: localization and ensemble size, verifying the impact of these parameters in the adaptive scheme. The adaptive ES-MDA used in this work defines the number of iterations and the inflation factors automatically and distance-based Kalman gain localization was used to evaluate the localization influence. The parameters influence was analyzed by applying the methodology in the benchmark UNISIM-I-H: a synthetic large-scale reservoir model based on an offshore Brazilian field. The experiments presented considerable reduction of the objective function for all cases, showing the ability of the adaptive methodology of keep iterating until a desirable overcome is obtained. About the parameters evaluated, a relationship between the localization and the required number of iterations to complete the adaptive algorithm was verified, and this influence has not been observed as function of the ensemble size.

Keywords: History Matching; Ensemble Smoother; Localization; Uncertainty Assessment.

RESUMO

RANAZZI, Paulo Henrique. **Análise dos Principais Parâmetros no Ajuste de Histórico utilizando ES-MDA adaptativo**. 2019. 81 p. Dissertação (Mestrado em Engenharia Mineral) – Escola Politécnica, Universidade de São Paulo, Santos, 2019.

Em engenharia de reservatórios, ajuste de histórico é a técnica que revisa os parâmetros incertos de um modelo de simulação de reservatório para obter uma resposta condizente com os dados de produção observados. As propriedades do reservatório possuem incertezas, devido aos métodos indiretos em que foram adquiridas, resultando em discrepâncias entre os dados observados e a resposta do simulador de reservatório. Um método de ajuste de histórico é o Conjunto Suavizado com Múltiplas Aquisições de Dados (sigla em inglês ES-MDA), onde um conjunto de modelos é utilizado para quantificar as incertezas dos parâmetros. No ES-MDA o número de iterações necessita ser definido previamente pelo usuário antes de sua aplicação, sendo um parâmetro determinante para um ajuste de boa qualidade. Uma forma de contornar esta limitação é implementar metodologias adaptativas onde o algoritmo continue as iterações até que alcance bons ajustes. Por outro lado, em modelos de reservatórios de larga-escala é necessário aplicar alguma técnica de localização para evitar correlações espúrias e uma alta redução de incertezas dos modelos a posteriori. O principal objetivo desta dissertação é avaliar dois principais parâmetros do ajuste de histórico quando aplicado um ES-MDA adaptativo: localização e tamanho do conjunto, verificando o impacto destes parâmetros no método adaptativo. O ES-MDA adaptativo utilizado define o número de iterações e os fatores de inflação automaticamente e a localização no ganho de Kalman baseada na distância foi utilizada para avaliar a influência da localização. Assim, a influência dos parâmetros foi analisada aplicando a metodologia no benchmark UNISIM-I-H: um modelo de reservatório sintético de larga escala baseado em um campo offshore brasileiro. Os experimentos apresentaram considerável redução da função objetivo para todos os casos, mostrando a capacidade da metodologia adaptativa de continuar iterando até que resultados aceitáveis fossem obtidos. Sobre os parâmetros avaliados, foi verificado uma relação entre a localização e o número de iterações necessárias, influência esta que não foi observada em função do tamanho do conjunto.

Palavras-chave: Ajuste de Histórico; Conjunto Suavizado; Localização; Quantificação de Incertezas.

LIST OF FIGURES

Figure 1 – EnKF sequential update workflow.	22
Figure 2 – ES simultaneous update workflow.....	24
Figure 3 – ES-MDA iterative workflow (Adapted from EnKF and ES workflows from Evensen (2007)).	25
Figure 4 – Shape of spherical and Gaussian covariance functions.	28
Figure 5 – (a) Gaspari and Cohn, (b) Furrer and Bengtsson with Spherical covariance function, (c) Furrer and Bengtsson with Gaussian covariance function.	28
Figure 6 – Methodology workflow.....	34
Figure 7 - Benchmark UNISIM-I-H.	39
Figure 8 - Averaged objective function evolution over the iterations for different ensemble sizes.	41
Figure 9 - Inflation factor evolution over the iterations for different ensemble sizes.....	41
Figure 10 - Well time series of (a) NA3D Oil Rate, (b) PROD023A Oil Rate, (c) NA3D Water Rate, (d) PROD023A Water Rate, (e) NA3D Bottom-hole Pressure, (f) PROD023A Bottom-hole Pressure.....	42
Figure 11 - Time series of injector well INJ010 and injector well INJ022.....	43
Figure 12 - First layer mean log-permeability in i-direction a before (prior) and after (posterior) the history matching for ensemble size equal to (b) 100, (c) 300, (d) 500.	43
Figure 13 - First layer log-permeability standard deviation in i-direction a before (prior) and after (posterior) the history matching for ensemble size equal to (b) 100, (c) 300, (d) 500	44
Figure 14 - Forecast period field cumulative oil production for ensemble size equal to (a) 100, (b) 300, (c) 500.	46
Figure 15 - Gaspari-Cohn correlation as a function of critical length.....	61
Figure 16 - Workflow of the adaptive ES-MDA plus Kalman gain localization.	62
Figure 17 - First layer grid top of UNISIM-I-H benchmark (wells projected).	63
Figure 18 - Values of ρ in the localization matrix for producer well NA3D and L = 2000 m.....	64

Figure 19 - Inflation factor evolution over iterations for different critical lengths.	65
Figure 20 - Time series of producer well NA3D. The gray lines represent the prior ensemble and the blue lines represent the posterior ensemble, red dots are the measurements.....	66
Figure 21 - Time series of producer well PROD023A. The gray lines represent the prior ensemble and the blue lines represent the posterior ensemble, red dots are the measurements.....	67
Figure 22 - Time series of water injector well INJ010. The gray lines represent the prior ensemble and the blue lines represent the posterior ensemble, red dots are the measurements.....	68
Figure 23 - Time series of water injector well INJ022. The gray lines represent the prior ensemble and the blue lines represent the posterior ensemble, red dots are the measurements.....	69
Figure 24 - Distribution of prior and posterior water-oil contact of the east block and rock compressibility.	70
Figure 25 - First layer log-permeability field in i-direction of the first realization before and after the assimilation for different critical lengths.....	70
Figure 26 - Normalized variance of prior and posterior models of log- permeability in i-direction for different critical lengths.	72

LIST OF TABLES

Table 1 - Measurement errors.	39
Table 2 – Forecast period controls.	40
Table 3 - Prior and posterior objective function values (mean \pm standard deviation), required number of iterations and the total required simulation runs (including the posterior ensemble) for different ensemble sizes.	41
Table 4 - Sum of normalized variance for different ensemble sizes.	45
Table 5 - Measurement errors in data assimilation used to construct the measurement errors matrix.	64
Table 6 - Mismatch of data and model objective functions (mean \pm standard deviation).	65

SUMMARY

ACKNOWLEDGEMENTS	3
ABSTRACT	7
RESUMO	9
LIST OF FIGURES	11
LIST OF TABLES	13
SUMMARY	15
CHAPTER 1 - INTRODUCTION	17
1.1 Objectives	19
1.2 Ensemble Methods	19
1.2.1 Kalman Filter (KF)	19
1.2.2 Ensemble Kalman Filter (EnKF)	21
1.2.3 Ensemble Smoother (ES)	22
1.2.4 Ensemble Smoother with Multiple Data Assimilation (ES-MDA)	24
1.3 Distance-based Kalman gain localization	26
1.4 Dissertation overview	28
CHAPTER 2 - ENSEMBLE SIZE INVESTIGATION IN ADAPTIVE ES-MDA	
RESERVOIR HISTORY MATCHING	31
2.1 Introduction	31
2.2 Methodology	33
2.2.1 Adaptive ES-MDA in the History Matching	34
2.2.2 Posterior Data Matching	38
2.2.3 Posterior Updated Models	38
2.3 Case Study	38
2.4 Results and Discussion	40
2.5 Conclusion	46
2.6 Acknowledgements	47

CHAPTER 3 - INFLUENCE OF THE KALMAN GAIN LOCALIZATION IN ADAPTIVE ENSEMBLE SMOOTHER HISTORY MATCHING	49
3.1 Introduction	49
3.2 Methodology.....	53
3.2.1 Adaptive ES-MDA	54
3.2.2 Objective Functions.....	59
3.2.3 Kalman Gain Localization	60
3.3 Case Study	62
3.4 Results of Assimilation of Production Data	65
3.5 Conclusions	72
3.6 Acknowledgments	73
CHAPTER 4 - CONCLUSIONS.....	75
4.1 Future Research.....	75
REFERENCES	77

CHAPTER 1 - INTRODUCTION

One of the most important tasks in the petroleum engineering is the forecast of the reservoir performance during its entire production life. The estimated reservoir behavior is used to define many production aspects, for example, flowlines, production platform settings, etc. Because of the computational advances, the most used tool to predict the reservoir behavior is the numerical reservoir simulation. The reservoir simulator is composed by a set of partial differential equations that represents the fluid flow through the reservoir (e.g. Darcy's law, Fourier law and Fick's laws of diffusion) (SANTOS, 2000). These equations are discretized in both space and time, and then, solved using numerical methods.

There are many properties used as input data to the construction of a simulation model, some examples are: porosity, permeability, fluid-contact depths, fault transmissibilities and fluid properties. These data are obtained through many acquisition sources, for example, core samples, well logs, rock and fluid laboratory tests, etc. These acquisition methods (most of them, indirect methods) can result in reservoir model description inaccuracies (uncertainties), and consequently, in errors in the numerical simulation (COATS, 1969). These errors can lead to a discrepancy between the simulator output and the measured (or observed) data, making it impractical to predict the future reservoir performance, since the model cannot reproduce the current behavior precisely. So, it is possible to conclude that reducing this discrepancy it will result in a reservoir forecast with better reliability. The process of modifying the uncertain reservoir parameters in order to reduce the discrepancy between the simulated and observed data is called history matching.

History matching can mathematically be generalized into two steps: forward and inverse problem. According to Tarantola (2005), the "forward problem" is a term used when a set of observable parameters \mathbf{d} (e.g., wells bottom-hole pressure, oil and water rates, etc.) is predicted as function of a set of model parameters \mathbf{m} (e.g., porosity, permeability, fluid contacts, etc.) and a forward operator \mathbf{g} (usually nonlinear):

$$\mathbf{d} = \mathbf{g}(\mathbf{m}) \quad (1)$$

and,

$$\mathbf{d} = [\text{BHP, OPR, WPR, GOR, etc}]^T \quad (2)$$

and,

$$\mathbf{m} = [\phi_1, \dots, \phi_m, k_{x_1}, \dots, k_{x_m}, k_{y_1}, \dots, k_{y_m}]^T \quad (3)$$

In reservoir engineering, the forward operator represents the numerical reservoir simulator, \mathbf{m} the uncertain reservoir parameters and \mathbf{d} the available observable data. History matching is an inverse problem: the model input is unknown (reservoir parameters) and the model output is known (measured reservoir production). So, the history matching can be described as the act of modifying \mathbf{m} in order to achieve a vector \mathbf{d} that corresponds with the measured data (the measured data is commonly named as \mathbf{d}_{obs}). Besides the parameters, the measurements also are subjected to uncertainties (TARANTOLA, 2005) that must be considered in the matching. Thus, it is clear that the main objective of history matching is to obtain a simulator response that corresponds to the measured reservoir behavior only approximately.

The matching can be divided into manual (trial and error) and automatic history matching. In the matching performed by trial and error, the reservoir engineer modifies only a subset of the uncertain parameters manually resulting in a single-matched model (RWECHUNGURA; DADASHPOUR; KLEPPE, 2011). The large cost of computing the reservoir simulator output makes the manual history matching approach impractical (OLIVER; REYNOLDS; LIU, 2008). History matching is considered an ill-posed problem because of the non-uniqueness of the solution, consequently, multiple combinations of the parameter values (often infinite combinations) can result in equally good matches (OLIVER; CHEN, 2011).

Clearly, the problem of finding \mathbf{m} that satisfies $\mathbf{d}_{\text{obs}} = \mathbf{g}(\mathbf{m})$, can be treated as an optimization problem, making possible an assisted approach. The concept of assisted history matching can be explained in the following steps: (1) Construction of a mathematical model; (2) Definition of an objective function; (3) Application of a minimization algorithm (RWECHUNGURA; DADASHPOUR; KLEPPE, 2011). Some examples of minimization algorithms are evolutionary algorithms, gradual deformation, neighborhood algorithm, gradients and adjoint methods, simultaneous perturbation stochastic approximation (SPSA), Kalman Filter methods, etc.

Oliver and Chen (2011) pointed out that Ensemble Kalman Filter (EnKF) is a history matching solution for realistic problems, but after their work several other

Kalman Filter methods were applied successfully in practical history matching problems. One of the most recent techniques used to perform the history matching process is the Ensemble Smoother with Multiple Data Assimilation (ES-MDA) (EMERICK; REYNOLDS, 2013). The ES-MDA is an iterative ensemble-based data-assimilation technique, it means that an ensemble of model realizations is used to represent the uncertainties in a model parameter estimation problem (SKJERVHEIM ET AL., 2011).

1.1 Objectives

The main objective of this dissertation is to apply an adaptive ES-MDA in a history matching problem of a large-scale reservoir model, in order to verify the impact of the main parameters in the adaptive assimilation scheme. Two important parameters were evaluated: (1) Ensemble size – the number of model realizations used; (2) Localization – weights in the assimilation according to the distance between the parameter and the data.

1.2 Ensemble Methods

In “Ensemble Methods”, an ensemble of models is used to represent and quantify the uncertain parameters and reservoir forecast. The following sections describe the basic theory of the Kalman Filter and the developments of the Ensemble Smoother with Multiple Data Assimilations (ES-MDA), algorithm used in this dissertation.

1.2.1 Kalman Filter (KF)

The Kalman Filter (KALMAN, 1960) is a recursive (sequential) estimator, optimal for linear models. In the forward step, both state \mathbf{y} and uncertainties \mathbf{P} (covariance) of the system are updated:

$$\mathbf{y}_{k+1} = \mathbf{F}\mathbf{y}_k \quad (4)$$

and,

$$\mathbf{P}_{k+1} = \mathbf{F}\mathbf{P}_k\mathbf{F}^T + \mathbf{Q} \quad (5)$$

where \mathbf{y} is the vector containing the uncertain parameters and state of the system, \mathbf{F} is the linear forward operator and \mathbf{Q} is the error covariance matrix for the model errors. These errors are assumed due to uncertainties in the forward models (physical modelling and numerical approximations) (EVENSEN, 2003). Equations 2 and 3 are then integrated forward in time to produce the forecast that will be corrected in the Kalman Filter analysis step in all times that contain available measurements before the integration continues (also called as sequential assimilation method):

$$\mathbf{y}^a = \mathbf{y}^f + \mathbf{P}^f \mathbf{H}^T (\mathbf{H} \mathbf{P}^f \mathbf{H}^T + \mathbf{C}_D)^{-1} (\mathbf{d}_{\text{obs}} - \mathbf{H} \mathbf{y}^f) \quad (6)$$

and,

$$\mathbf{P}^a = \mathbf{P}^f - \mathbf{P}^f \mathbf{H}^T (\mathbf{H} \mathbf{P}^f \mathbf{H}^T + \mathbf{C}_D)^{-1} \mathbf{H} \mathbf{P}^f \quad (7)$$

where \mathbf{H} is the measurement operator that relates the model state to the observations considering the measurement errors, \mathbf{C}_D is the covariance matrix for the measurement errors, f represent forecast and a represent analysis. The term $\mathbf{P}^f \mathbf{H}^T (\mathbf{H} \mathbf{P}^f \mathbf{H}^T + \mathbf{C}_D)^{-1}$ is also called “Kalman gain matrix”.

$$\mathbf{K} = \mathbf{P}^f \mathbf{H}^T (\mathbf{H} \mathbf{P}^f \mathbf{H}^T + \mathbf{C}_D)^{-1} \quad (8)$$

If the measurements are uncorrelated, the covariance matrix will be the diagonal matrix:

$$\mathbf{C}_D = \begin{bmatrix} \sigma_1^2 & 0 & \dots & 0 \\ 0 & \sigma_2^2 & & \vdots \\ \vdots & & \ddots & 0 \\ 0 & \dots & 0 & \sigma_{N_d}^2 \end{bmatrix} \quad (9)$$

being σ the standard deviation of each measurement error and N_d the number of measurements of the system.

For large models, the cost of upgrading the model covariance (Equation 5) matrix is extremely large, what makes it impracticable. Also, for nonlinear models, linearization of the model is required for updating the covariance. The Extended Kalman Filter uses the tangent linear operator of the nonlinear model to represent \mathbf{F} in Equation 9 (EVENSEN, 2003), however this linearization is not suitable for large models.

1.2.2 Ensemble Kalman Filter (EnKF)

To overcome the difficulties of the KF in nonlinear and large models, Evensen (1994, 2003) proposed the Ensemble Kalman Filter (EnKF). The main feature of the EnKF is the use of an ensemble of models to represent the uncertainties and compute the covariance of the system (avoiding the calculation of Equation 3). Denoting j as the index for the j th member of the N_e -size ensemble, and \mathbf{g} being the nonlinear forward operator (as described in the previous forward problem definition), the forward step of all members in the EnKF can be defined as:

$$\mathbf{y}_{j,k+1} = \mathbf{g}(\mathbf{y}_{j,k}) \quad (10)$$

where $j = 1, \dots, N_e$. So, the covariances are estimated around the ensemble mean of the state (EVENSEN, 2003):

$$\mathbf{P}^f \cong \mathbf{P}_e^f = \overline{(\mathbf{y}^f - \bar{\mathbf{y}}^f)(\mathbf{y}^f - \bar{\mathbf{y}}^f)^T} \quad (11)$$

and,

$$\mathbf{P}^a \cong \mathbf{P}_e^a = \overline{(\mathbf{y}^a - \bar{\mathbf{y}}^a)(\mathbf{y}^a - \bar{\mathbf{y}}^a)^T} \quad (12)$$

where the overbars denote the ensemble mean. The analysis step in the EnKF follows for all ensemble members:

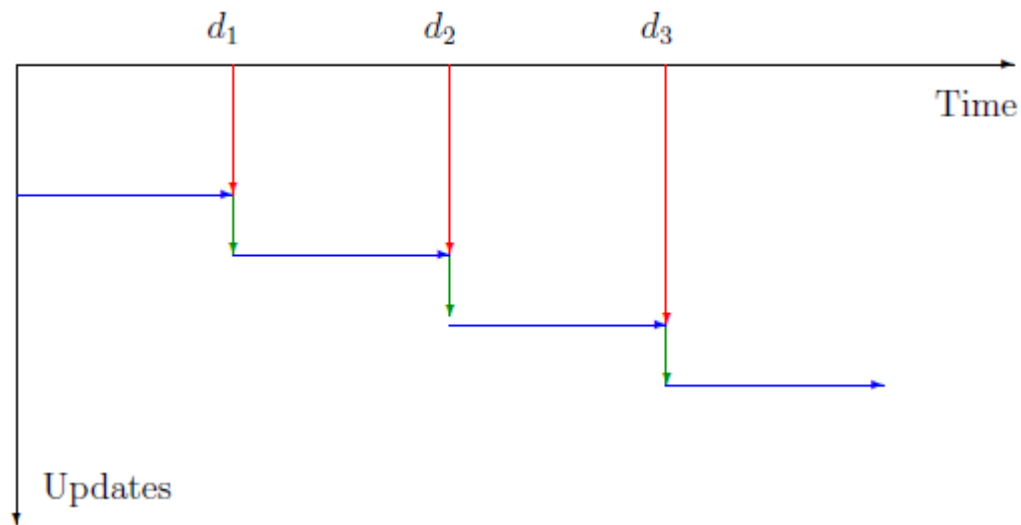
$$\mathbf{y}_j^a = \mathbf{y}_j^f + \mathbf{P}_e^f \mathbf{H}^T (\mathbf{H} \mathbf{P}_e^f \mathbf{H}^T + \mathbf{C}_D)^{-1} (\mathbf{d}_{\text{obs},j} - \mathbf{H} \mathbf{y}_j^f) \quad (13)$$

Burgers, van Leeuwen and Evensen (1998) pointed out the necessity to treat the observations as random variables in the EnKF. So, the ensemble of observations can be defined as:

$$\mathbf{d}_{\text{obs},j} = \mathbf{d}_{\text{obs}} + \varepsilon_j \quad (14)$$

being $\mathbf{C}_D = \overline{\varepsilon \varepsilon^T}$ as the ensemble goes to infinity. Figure 1 shows the sequential update procedure used in the EnKF. The blue arrows represent the forward step (Equations 7 and 9). The green arrows represent the EnKF recursive updates (Equations 9 and 10) with the available measurements represented by the red arrows.

Figure 1 – EnKF sequential update workflow.



Source: Evensen (2007).

In the first application of EnKF to update the uncertain reservoir parameters in the petroleum engineer, Nævdal, Mannseth and Vefring (2002) applied the EnKF to continuous update only the near-well permeability in a simple reservoir model. After this, Nævdal et al. (2003) applied the EnKF in two examples: a synthetic case and a simplified field model to update the permeability of the entire reservoir model. Since then, EnKF and variants have been applied in the practical history matching problems, for example, Zafari and Reynolds (2005), Seiler et al. (2009), Zhang and Oliver (2011), Heidari et al. (2013), Shuai et al. (2016), Xu et al. (2018).

The recursive methodology of the EnKF can lead to some issues during the application in history matching. Some issues can occur due to the simulations restarts and the necessity of update the state variables (e.g. pressure and saturation in all gridblocks) at each assimilation step. The restarts can lead to a large computational effort and the state updates can result in inconsistencies between parameter and state (leading to spurious correlations and nonphysical values).

1.2.3 Ensemble Smoother (ES)

The Ensemble Smoother (ES) is a simultaneous assimilation variant of the EnKF, proposed by van Leeuwen and Evensen (1996) as an alternative to avoid the recursive updates and state updates. The ES update has the same form than EnKF updates, with the difference that all data are assimilated simultaneously in a single update step. The single ES update also makes unnecessary the state updates: the

forward step of the updated ensemble runs again from time zero with the initial state of the system (Figure 2). So, the ES can be treated as a parameter estimation problem:

$$\mathbf{d}_j^f = \mathbf{g}(\mathbf{m}_j^f) \quad (15)$$

where \mathbf{m} represents only the uncertain parameters of the model. Using the definition of parameter estimation problem, the analysis step in ES can be defined for all ensemble members as:

$$\mathbf{m}_j^a = \mathbf{m}_j^f + \mathbf{P}_e^f \mathbf{H}^T (\mathbf{H} \mathbf{P}_e^f \mathbf{H}^T + \mathbf{C}_D)^{-1} (\mathbf{d}_{\text{obs},j} - \mathbf{d}_j^f) \quad (16)$$

Avoiding the use of the measurement operator, the matrices $\mathbf{P}_e^f \mathbf{H}^T$, $\mathbf{H} \mathbf{P}_e^f \mathbf{H}^T$ can be represented in such form:

$$\mathbf{P}_e^f \mathbf{H}^T = \mathbf{C}_{\text{MD}}^f \quad (17)$$

and,

$$\mathbf{H} \mathbf{P}_e^f \mathbf{H}^T = \mathbf{C}_{\text{DD}}^f \quad (18)$$

Then, the covariances can be estimated as:

$$\mathbf{C}_{\text{MD}}^f = \overline{(\mathbf{m}^f - \bar{\mathbf{m}}^f)(\mathbf{d}^f - \bar{\mathbf{d}}^f)^T} = \frac{1}{N_e - 1} \sum_{j=1}^{N_e} (\mathbf{m}_j^f - \bar{\mathbf{m}}^f)(\mathbf{d}_j^f - \bar{\mathbf{d}}^f)^T \quad (19)$$

and,

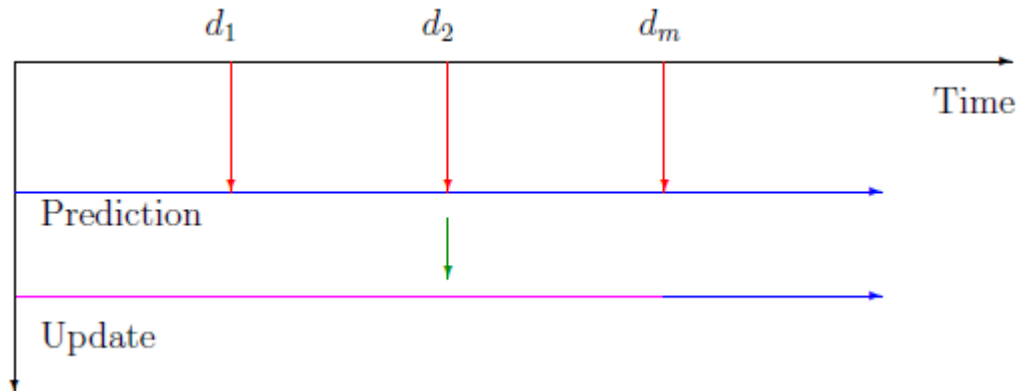
$$\mathbf{C}_{\text{DD}}^f = \overline{(\mathbf{d}^f - \bar{\mathbf{d}}^f)(\mathbf{d}^f - \bar{\mathbf{d}}^f)^T} = \frac{1}{N_e - 1} \sum_{j=1}^{N_e} (\mathbf{d}_j^f - \bar{\mathbf{d}}^f)(\mathbf{d}_j^f - \bar{\mathbf{d}}^f)^T \quad (20)$$

So, the analysis equation of ES becomes:

$$\mathbf{m}_j^a = \mathbf{m}_j^f + \mathbf{C}_{\text{MD}}^f (\mathbf{C}_{\text{DD}}^f + \mathbf{C}_D)^{-1} (\mathbf{d}_{\text{obs},j} - \mathbf{d}_j^f) \quad (21)$$

Figure 2 shows the simultaneous update procedure used in the ES. The blue arrow represents the forward step over all time domain that contains measurements. The green arrow represents the single update containing all available measurements represented by the red arrows. The magenta arrow represents the forecast after the data assimilation.

Figure 2 – ES simultaneous update workflow.



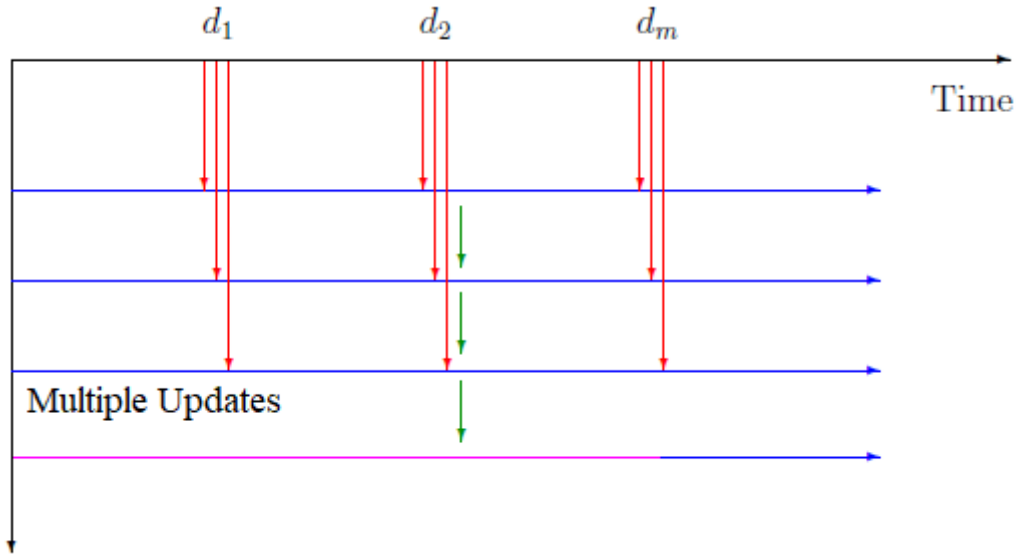
Source: Evensen (2007).

In the first ES application in history matching, Skjervheim et al. (2011) pointed out that ES has easier implementation in comparison with EnKF because of the parameter estimation methodology. Besides that, they concluded that computationally, ES is much faster than EnKF because of the lack of the simulation restarts. On the other hand, the single analysis without the state updates reduces the quality of the results, especially for strongly nonlinear systems, requiring iterative methods to improve the assimilation (MA et al., 2017).

1.2.4 Ensemble Smoother with Multiple Data Assimilation (ES-MDA)

To improve the results keeping the problem as a parameter estimation problem using a smoother formulation, Emerick and Reynolds (2013) proposed the Ensemble Smoother with Multiple Data Assimilation (ES-MDA). The ES-MDA method assimilates all observed data multiple times using the same ES analysis formulation, with the addition of an inflation factor on the covariance for the measurement errors (C_D matrix). The objective of the inflation factor is to damp the changes in the parameters at each iteration. Emerick and Reynolds (2013) define the ES-MDA iterations as Gauss-Newton steps, so the ES-MDA perform multiple smaller corrections over the model parameters instead of the single and larger ES update. Figure 3 shows the multiple data assimilation procedure in the ES-MDA. The blue arrows represent the forward step for all iterations. The green arrows represent the damped updates containing all available measurements represented by the red arrows. The magenta arrow represents the forecast after the data assimilation.

Figure 3 – ES-MDA iterative workflow (Adapted from EnKF and ES workflows from Evensen (2007)).



Because of the iterative methodology, it is convenient to change the terms “forecast” and “analysis” for an iteration index. So, the analysis equation in the ES-MDA is represented as:

$$\mathbf{m}_j^{i+1} = \mathbf{m}_j^i + \mathbf{C}_{MD}^i (\mathbf{C}_{DD}^i + \alpha_i \mathbf{C}_D)^{-1} (\mathbf{d}_{obs,j}^i - \mathbf{d}_j^i) \quad (22)$$

where α is the inflation factor. In ES-MDA the inflation factor is used to create the measurements perturbations. A convenient form to create the measurement ensemble is:

$$\mathbf{d}_{obs,j}^i = \mathbf{d}_{obs} + \sqrt{\alpha_i} \mathbf{C}_D^{1/2} \mathbf{z}_j \quad (23)$$

where \mathbf{z}_j is a Gaussian sample with mean zero and covariance equal to one ($\mathbf{z}_j \sim \mathcal{N}(0, \mathbf{I}_{N_d})$). Chapter 2 and Chapter 3 detail the algorithm and workflow to apply the ES-MDA in history matching.

In ES-MDA the number of iterations that will be performed, as the inflation factor of each iteration need to be defined by the user before the start of the algorithm. Emerick and Reynolds (2013) defined the equivalence between the single assimilation (ES) and the multiple data assimilation method (ES-MDA) for the linear Gaussian case. The following condition must be held to keep the equivalence and guarantee the correct posterior distribution:

$$\sum_{i=1}^{N_i} \alpha_i^{-1} = 1 \quad (24)$$

where N_i represent the total number of iterations (or assimilations). Analyzing Equation 24, it is possible to conclude that infinite inflation factors combinations can be defined over the iterations. Since then, many practical history matching problems using ES-MDA were performed using the same inflation factor for all iterations ($[\alpha_1, \dots, \alpha_{N_i}] = N_i$). Some examples are: Emerick (2018), Ranazzi and Sampaio (2018), Silva et al. (2018), Soares, Maschio and Schiozer (2018).

An important question that need to be commented is the fact if the results obtained after the ES-MDA application are not desirable, it is necessary to restart the entire algorithm with a different number of iterations and inflation factor at each iteration, requiring a large computation effort and time spent. The manual selection of the inflation factors and the number of iterations required for the ES-MDA lead to the development of adaptive methodologies. The main concept of the adaptive methodologies is to perform the selection of both parameters automatically, consequently, these algorithms keep iterating until it reaches low objective function values. Thus, the development of adaptive methodologies has become the nowadays researches goal.

1.3 Distance-based Kalman gain localization

In large-scale models the number of uncertain parameters is very higher than the number of ensemble members used in the algorithm. This can lead to a bad representation of the covariances in ensemble methods (the matrices \mathbf{C}_{MD}^i and \mathbf{C}_{DD}^i), resulting in extreme posterior variance reduction of the uncertain parameters (this reduction is also called as “Ensemble Collapse”). One way to avoid these sampling errors is to perform a localization technique that restricts the assimilation influence between the uncertain parameters and data. According to Chen and Oliver (2016), the localization of the Kalman gain matrix have become the state-of-art for history matching applications.

The application of Kalman gain localization consists in use a localization matrix to weight the Kalman gain matrix, using the Schur (element-wise) product. So, the Analysis equation using the Kalman gain localization can be represented as:

$$\mathbf{m}_j^{i+1} = \mathbf{m}_j^i + \rho \circ \left[\mathbf{C}_{MD}^i (\mathbf{C}_{DD}^i + \alpha_i \mathbf{C}_D)^{-1} \right] (\mathbf{d}_{\text{obs},j}^i - \mathbf{d}_j^i) \quad (25)$$

where ρ represents the localization matrix and \circ denotes the Schur product. So, it is clear to describe the localization matrix as the weighting between each pair parameter-data:

$$\rho = \begin{bmatrix} \rho_{m_1,d_1} & \rho_{m_1,d_2} & \cdots & \rho_{m_1,d_{N_d}} \\ \rho_{m_2,d_1} & \rho_{m_2,d_2} & & \rho_{m_2,d_{N_d}} \\ \vdots & & \ddots & \vdots \\ \rho_{m_{N_m},d_1} & \rho_{m_{N_m},d_2} & \cdots & \rho_{m_{N_m},d_{N_d}} \end{bmatrix} \quad (26)$$

The main concept of the distance-based localization is to restrict the assimilation, introducing weights based on the distance between each parameter and data through a correlation function. One widely used correlation function is the Gaspari and Cohn correlation (GASPARI; COHN, 1999), that calculates the weight based on the Euclidian distance between the parameter and data and a critical length:

$$\rho(z) = \begin{cases} -\frac{1}{4}\left(\frac{z}{L}\right)^5 + \frac{1}{4}\left(\frac{z}{L}\right)^4 + \frac{5}{8}\left(\frac{z}{L}\right)^3 - \frac{5}{3}\left(\frac{z}{L}\right)^2 + 1, & 0 \leq z \leq L \\ \frac{1}{12}\left(\frac{z}{L}\right)^5 - \frac{1}{2}\left(\frac{z}{L}\right)^4 + \frac{5}{8}\left(\frac{z}{L}\right)^3 + \frac{5}{3}\left(\frac{z}{L}\right)^2 - 5\left(\frac{z}{L}\right) + 4 - \frac{2}{3}\left(\frac{L}{z}\right) & L \leq z \leq 2L \\ 0, & 2L \leq z \end{cases} \quad (27)$$

where z is the Euclidian distance and L represents the critical length. Another example of correlation function is the Furrer and Bengtsson correlation (FURRER; BENGTTSSON, 2007). In this correlation, the weights are determined as function of a covariance function and the ensemble size, in such a way that the larger the ensemble, larger the influence of the measurements (CHEN; OLIVER, 2016):

$$\rho(z) = \frac{1}{1 + [1 + f(0)^2/f(z)^2]/N_e} \quad (28)$$

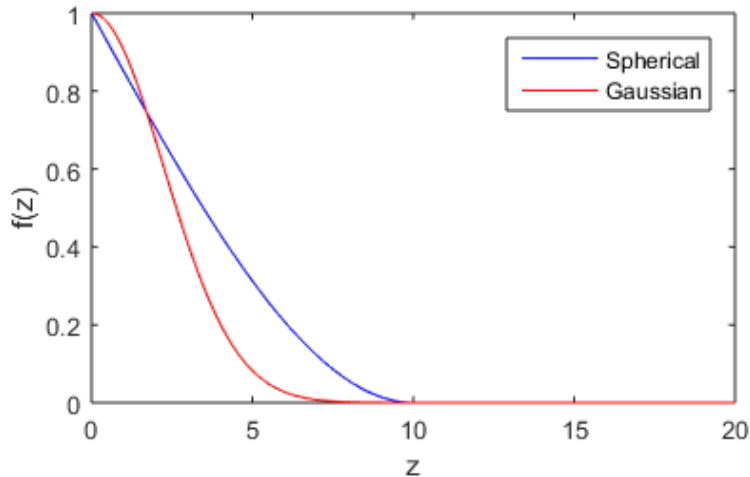
where f represents a covariance function. Some examples of covariance functions that can be used are spherical (for localization purposes, b is set equal to one to maintain the weights between 0 and 1, Figure 4 shows the shape of both covariance functions):

$$f_{spherical}(z) = \begin{cases} b \left(1 - \frac{3|z|}{2L} + \frac{1}{2} \frac{|z|^3}{L^3} \right), & 0 \leq z \leq L \\ 0, & L < z \end{cases} \quad (29)$$

and Gaussian:

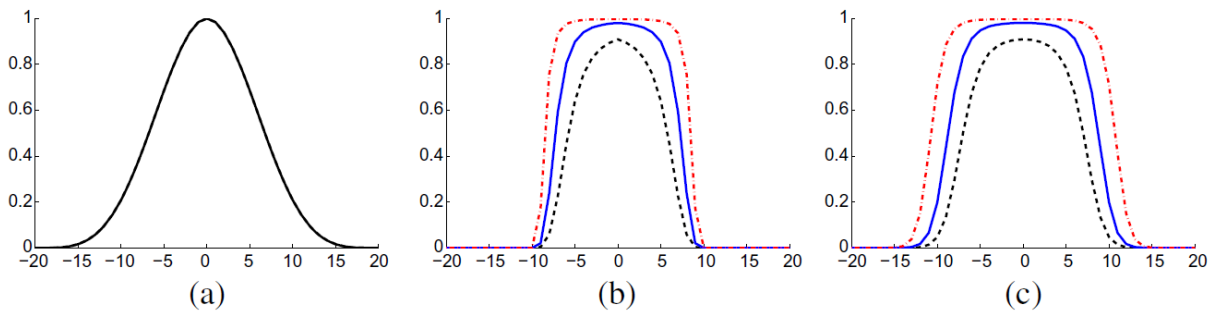
$$f_{Gaussian}(z) = b \cdot \exp\left(-\frac{|z|^2}{L}\right) \quad (30)$$

Figure 4 – Shape of spherical and Gaussian covariance functions.



Chen and Oliver (2016) investigated both correlations functions mentioned above. Figure 5 shows the shape of both correlations as function of the Euclidian distance for a critical length equal to 10. In Furrer and Bengtsson correlation, the black dashed lines represent ensemble size of 20, blue solid lines represent ensemble size of 100 and red dash-dotted lines represent ensemble size of 1000.

Figure 5 – (a) Gaspari and Cohn, (b) Furrer and Bengtsson with Spherical covariance function, (c) Furrer and Bengtsson with Gaussian covariance function.



Source: Chen and Oliver (2016).

1.4 Dissertation overview

This dissertation consists of four chapters that are related to each other through the application of the adaptive ES-MDA methodology in the benchmark UNISIM-I-H: a large-scale synthetic reservoir simulation model, based on a Brazilian real field.

Chapter 2 presents the ensemble size investigation in the adaptive ES-MDA. The fact that the number of model realizations have major influences in the uncertainty

assessment in ensemble-based methods is one well-known role in the history matching community. However, we did not find anything about this influence in adaptive methodologies. In this chapter, we presented the algorithm of the adaptive ES-MDA proposed by Emerick (2016) and some information about other adaptive variants developed. Then, the investigation was made varying the ensemble size (from 100 to 500) with the other parameters fixed. As expected, the larger ensembles presented better variance of the posterior models. However, the ensemble size does not showed influences on the number of iterations and the inflation factor selection. The full text from Chapter 2 has been submitted in the *Journal of the Brazilian Society of Mechanical Sciences and Engineering*.

Chapter 3 examines the influence of the Kalman gain localization in the adaptive ES-MDA. Motivated by Chen and Oliver (2016), that pointed out that all localization methods gave equivalent results when it is applied with iterative forms of ES, we bring up the following question: is there any influence when the localization is applied with adaptive forms of ES? In Chapter 3, we provided a robust description of the adaptive ES-MDA proposed by Emerick (2016), including the ensemble representation and the subspace inversion procedure. We performed this combining the work of Emerick (2016) and some valuable information from Evensen (2004), providing useful information for the methodology implementation. The localization was analyzed applying the Gaspari and Cohn correlation changing the critical length. The critical length showed influences on the number of iterations required to the algorithm completion, as can be seen when the lowest critical length in the study ($L = 1000$ m) resulted in a high number of iterations (that greatly increases the total computational time) to complete the algorithm, and in addition presenting worse data matchings. The full text from Chapter 3 was published as a full manuscript by the *Journal of Petroleum Science and Engineering*.

CHAPTER 2 - ENSEMBLE SIZE INVESTIGATION IN ADAPTIVE ES-MDA RESERVOIR HISTORY MATCHING

Abstract

In this work, we study the ensemble size influence on an adaptive ensemble-based methodology for history matching of petroleum reservoirs. The assimilation scheme used is an adaptive Ensemble Smoother with Multiple Data Assimilation (ES-MDA) in which both the total number of assimilations and the inflation factor of each iteration are defined automatically by the algorithm. This fact leads to the assumption that the predefined algorithm parameters may have influence in the total number of assimilations and the inflation factors. One main parameter that can be investigated is the number of ensemble members used in the assimilation, also called ensemble size. The ensemble size influence was analyzed by applying the adaptive ES-MDA in a synthetic large-scale reservoir model. As result of the investigation, the ensemble size showed influence on the reduction of the uncertainty of the posterior models, but it did not show any influence on the total number of assimilations and on the inflation factor selection.

2.1 Introduction

History matching is the data assimilation process that modifies the uncertain parameters of a simulation reservoir model. The objective is to obtain a simulation response equivalent to the available production data, improving the simulation model reliability and, consequently, providing a better forecast of the future performance of the reservoir. Aanonsen et al. (2009), Oliver and Chen (2011) and Rwechungura, Dadashpour and Kleppe (2011) review the techniques and the recent advances in the history matching, most of them associated with the application of the Ensemble Kalman Filter (EnKF). The EnKF is a Monte Carlo sequential assimilation method developed by Evensen (1994, 2003), where an ensemble of model realizations is used to represent the uncertainty. This ensemble is integrated forward in time (called the forward step), and the uncertain parameters and state variables (e.g. pressure and saturation) are “corrected” recursively whenever measurements are available in a parameter-state estimation problem (called the analysis or assimilation step) (EVENSEN, 2003). There are several EnKF applications in history matching (e.g.,

Haugen et al. (2008), Zhang and Oliver (2011), Heidari et al. (2013) and Shuai et al. (2016)), however its necessity to update the state in each analysis step can lead to a high computational effort and statistical inconsistencies between the parameter and state (THULIN et al., 2007, 2011; WANG; LI; REYNOLDS, 2010). Due to this, techniques based on the Ensemble Smoother (ES), developed by van Leeuwen and Evensen (1996) have become the state-of-art in history matching. In smoother techniques, all available data are assimilated simultaneously in a single step, avoiding the state updates during the assimilation (being a parameter estimation problem). For nonlinear problems, the single ES update is not enough to provide satisfactory matchings, requiring iterative methods to improve the assimilation (MA et al., 2017). An iterative method that has become popular is the Ensemble Smoother with Multiple Data Assimilation (ES-MDA), developed by Emerick and Reynolds (2013). The ES-MDA is an iterative assimilation scheme that uses the same ES formulation, assimilating the same data multiple times (in multiple assimilation steps, or iterations) with the addition of an inflation factor in order to damp each iteration. There are several ES-MDA applications in large-scale reservoirs history matching, e.g., Maucec et al. (2016), Breslavich, Sarkisov and Marakova (2017), Emerick (2016), and Morosov and Schiozer (2017). The necessity of define the number of iterations and the inflation factors before the assimilation process is one of the main drawbacks of the ES-MDA in your standard form: it is necessary restart the entire process if the results quality is not desirable after the end of the algorithm. Moreover, some works conclude that the correct selection of the inflation factors can improve the assimilation process (LE; EMERICK; REYNOLDS, 2016; RAFIEE; REYNOLDS, 2017). Evensen (2018) concludes that this improvement due the inflation factor selection could be obtained when a low number of iterations in the ES-MDA is used. The development of adaptive methodologies, when the number of iterations and the inflation factors are defined automatically, has become the nowadays researches goal. Some adaptive algorithms based on the ES-MDA were developed. Iglesias (2015) proposed a derivative-free iterative regularizing Ensemble Smoother (IR-ES). Le, Emerick and Reynolds (2016) proposed two adaptive variants of ES-MDA: one with a heuristical restricted step (ES-MDA-RS), and another with a regularizing Levenberg-Marquardt scheme (ES-MDA-RLM). It is important to point out that both IR-ES and ES-MDA-RLM are based on the discrepancy principle for the choice of the inflation factors (or the step length). Rafiee and Reynolds (2017) proposed a procedure to choose the inflation factors within a

predetermined number of iterations, where the inflation factors decrease geometrically with iteration number (ES-MDA-GEO). The selection of the number of iterations before the assimilation can be an advantage when the computational effort is limited, but this allow to a suboptimal selection of the number of iterations. Emerick (2016) proposed an adaptive variant of the ES-MDA (adapt. ES-MDA) where the inflation factor of each iteration is related with a normalized objective function that measures the discrepancy between the simulator response and the data, defining only a maximum inflation factor allowed in the iterations. This algorithm keeps iterating until it reaches low discrepancies (being the number of iterations and the inflation factor defined automatically).

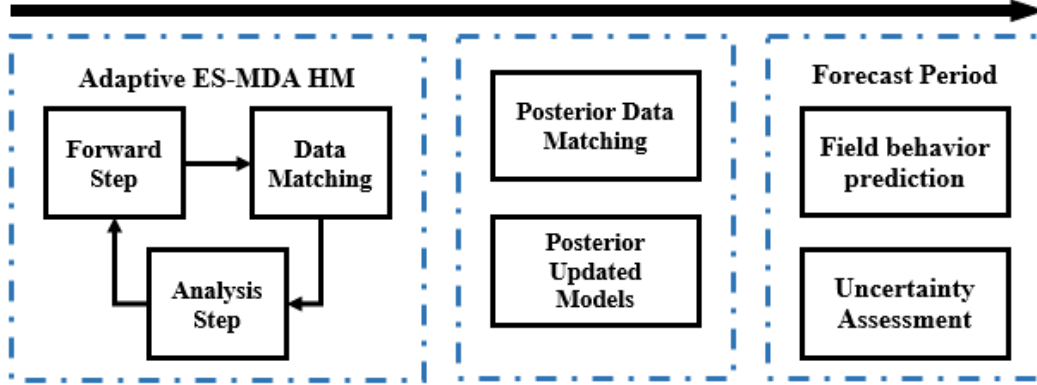
In this work, we will investigate the influence of the ensemble size in the adaptive ES-MDA proposed by Emerick (2016) when it is applied in a large-scale reservoir simulation model. We chose this methodology because either the number of iterations and the inflation factors are defined automatically. The case study selected to check the ensemble influence is the benchmark UNISIM-I, since some works already performed history matching in UNISIM-I using the ES-MDA (e.g., Morosov and Schiozer (2017), Silva et al. (2017), Soares, Maschio and Schiozer (2018), Emerick (2018), Ranazzi and Sampaio (2018)). In Ranazzi and Sampaio (2019), the influence of the localization was verified in the adaptive scheme, where lower correlation lengths resulted in more required iterations to perform the entire algorithm. In Section 2.2, we define the history matching problem and the adaptive ES-MDA methodology, in Section 2.3 we describe the benchmark UNISIM-I and the experiments that we run to the discussion. Then, in Section 2.4, we present the results obtained to discuss the ensemble size influence in the adaptive ES-MDA.

2.2 Methodology

The ensemble size investigation was performed by running the adaptive ES-MDA methodology for different ensemble sizes, and the comparison will be made through several approaches. The algorithm was implemented in MATLAB®, combining the iterative forward steps (IMEX simulator of CMG ®) and the analysis steps (adaptive ES-MDA). The following sections will introduce the adaptive ES-MDA methodology for history matching (EMERICK, 2016) and the objective functions used to evaluate the matching in terms of data and model parameters. Figure 6 shows the methodology

workflow used in this study, that consists in the following steps: history matching, analysis of the posterior models and analysis of the forecast production period.

Figure 6 – Methodology workflow.



2.2.1 Adaptive ES-MDA in the History Matching

In ensemble-based methods, each member j is used to represent the ensemble with size N_e . The uncertain reservoir parameters can be composed of permeabilities in different directions, porosity, net-to-gross ratio, fluid contacts, fault transmissibility multipliers, etc. (CHEN; OLIVER, 2010). In the history matching problem, it is convenient to collect all the N_m uncertain parameters into a vector \mathbf{m} :

$$\mathbf{m}_j = [m_{1,j}, m_{2,j}, \dots, m_{N_m,j}]^T \in \mathcal{R}^{N_m}. \quad (31)$$

Also, all the N_d the simulator response and the observed data that will be matched (e.g., production and injection rates, bottom-hole pressure in different time periods, etc.) can be collected into the vectors \mathbf{d} and \mathbf{d}_{obs} , respectively:

$$\mathbf{d}_j = [d_{1,j}, d_{2,j}, \dots, d_{N_d,j}]^T \in \mathcal{R}^{N_d}, \quad (32)$$

and,

$$\mathbf{d}_{\text{obs}_j} = [d_{\text{obs}_{1,j}}, d_{\text{obs}_{2,j}}, \dots, d_{\text{obs}_{N_d,j}}]^T \in \mathcal{R}^{N_d} \quad (33)$$

The forward step relates the uncertain parameters vector with the simulator response:

$$\mathbf{d}_j = \mathbf{g}(\mathbf{m}_j) \quad (34)$$

where g is the forward operator (in the history matching, the reservoir flow simulator). The main objective of the history matching problem is to reduce the discrepancy

between the simulated and observed (measured) data. This discrepancy can be represented through an objective function, one well-known objective function is (EMERICK, 2016; LE; EMERICK; REYNOLDS, 2016):

$$O_{Na,j} = \frac{1}{2N_d} (\mathbf{d}_j^i - \mathbf{d}_{\text{obs}})^T \mathbf{C}_D^{-1} (\mathbf{d}_j^i - \mathbf{d}_{\text{obs}}), \quad (35)$$

where \mathbf{C}_D is the covariance of measurement errors. If the data are uncorrelated, \mathbf{C}_D is assumed to be diagonal (EMERICK, 2016) (where σ represents the standard deviation of each measurement):

$$\mathbf{C}_D = \begin{bmatrix} \sigma_1^2 & 0 & \cdots & 0 \\ 0 & \sigma_2^2 & & \vdots \\ \vdots & & \ddots & 0 \\ 0 & \cdots & 0 & \sigma_{N_d}^2 \end{bmatrix} \in \mathfrak{R}^{N_d \times N_d} \quad (36)$$

The analysis equation for each ensemble member j and iteration i in the ES-MDA can be expressed as:

$$\mathbf{m}_j^{i+1} = \mathbf{m}_j^i + \mathbf{C}_{\text{MD}}^i (\mathbf{C}_{\text{DD}}^i + \alpha_i \mathbf{C}_D)^{-1} (\mathbf{d}_{\text{obs},j}^i - \mathbf{d}_j^i), \quad (37)$$

where \mathbf{C}_{MD} is the cross-covariance between the parameters and the simulated data, \mathbf{C}_{DD} is the auto-covariance of the simulated data, α_i is the inflation factor (or step length) for iteration i and $\mathbf{d}_{\text{obs},j}^i$ is the perturbed measured data. In the ES-MDA methodology, the measurements must be treated as random variables to maintain the correct variance after the analysis (BURGERS; VAN LEEUWEN; EVENSEN, 1998; CHEN; OLIVER, 2010), creating the ensemble of observations $\mathbf{d}_{\text{obs},j}^i$, adding to the original measurements a Gaussian white noise with covariance $\alpha_i \mathbf{C}_D$:

$$\mathbf{d}_{\text{obs},j}^i \sim \mathcal{N}(\mathbf{d}_{\text{obs}}, \alpha_i \mathbf{C}_D). \quad (38)$$

Also, in ES-MDA the covariances are estimated around the ensemble mean:

$$\mathbf{C}_{\text{MD}}^i = \frac{1}{N_e - 1} \sum_{j=1}^{N_e} (\mathbf{m}_j^i - \bar{\mathbf{m}}^i) (\mathbf{d}_j^i - \bar{\mathbf{d}}^i)^T \in \mathfrak{R}^{N_m \times N_d}, \quad (39)$$

and

$$\mathbf{C}_{\text{DD}}^i = \frac{1}{N_e - 1} \sum_{j=1}^{N_e} (\mathbf{d}_j^i - \bar{\mathbf{d}}^i) (\mathbf{d}_j^i - \bar{\mathbf{d}}^i)^T \in \mathfrak{R}^{N_d \times N_d}, \quad (40)$$

where the overbars denote the ensemble mean.

2.2.1.1 Inflation Factors Selection in the Adaptive ES-MDA

Emerick and Reynolds (2013) demonstrated that ES-MDA is equivalent to ES (for the linear-gaussian case) only if the following condition holds:

$$\sum_{i=1}^{N_i} \alpha_i^{-1} = 1. \quad (41)$$

A common way to select the inflation factor is set $\alpha_i = N_i$ for all iterations (e.g., Silva et al. (2017), Soares, Maschio and Schiozer (2018), Emerick (2018)). Making the assumption that one ES-MDA iteration is equivalent with one Gauss-Newton iteration, it is possible to conclude that lower lengths at initial steps (higher inflation factors at early iterations) can improve the assimilation process, avoiding overcorrections (LE; EMERICK; REYNOLDS, 2016). On the other hand, the discrepancy between the simulator response and the observed data decreases during the history matching process, so, Emerick (2016) proposed an adaptive ES-MDA where the user only defines a maximum inflation factor α_{\max} , a maximum number of iterations i_{\max} and a heuristical factor that relates the inflation factor of each iteration and the discrepancy measured through an objective function (in this case, the averaged objective function \bar{O}_{Nd}^i). The inflation factor of each iteration is computed as:

$$\alpha_i = \min\{a\bar{O}_{Nd}^i, \alpha_{\max}\}, \quad (42)$$

where a ($a > 0$) is the heuristical factor that relates the step length and the discrepancy.

The averaged objective function can be defined as:

$$\bar{O}_{Nd}^i = \frac{1}{N_e} \sum_{j=1}^{N_e} O_{Nd,j}^i. \quad (43)$$

To hold the condition of Eq. 41, after the definition of the iteration length size (before the analysis at each iteration) the following conditions must be checked:

$$\sum_{i=1}^{N_i} \alpha_i^{-1} > (1 - \alpha_{\max}^{-1}) \text{ or } i = i_{\max}. \quad (44)$$

If any condition is violated, a new inflation factor must be calculated using Eq. 41, then, the last analysis step is performed. The algorithm of the adapt. ES-MDA is as follows:

For each iteration:

1. Run the forward model for every ensemble member from time zero

$$\mathbf{d}_j^i = g(\mathbf{m}_j^i).$$

2. Compute:

$$\bar{O}_{N_d}^i = (1/N_e) \sum_{j=1}^{N_e} (1/2N_d) (\mathbf{d}_j^i - \mathbf{d}_{\text{obs}})^T \mathbf{C}_D^{-1} (\mathbf{d}_j^i - \mathbf{d}_{\text{obs}}).$$

3. Define step length:

$$\alpha_i = \min\{a\bar{O}_{N_d}^i, \alpha_{\text{max}}\}.$$

4. Check condition:

$$\sum_{i=1}^{N_i} \alpha_i^{-1} > (1 - \alpha_{\text{max}}^{-1}) \text{ or } i = i_{\text{max}}.$$

5. If any condition is violated:

- Calculate a new inflation factor for Eq. 41 setting equal to one:

$$\sum_{i=1}^{N_i} \alpha_i^{-1} = 1.$$

- Perform last iteration (Step 7 and Step 8); then, terminate the algorithm.

6. end (if)

7. Perturb measurements:

$$\mathbf{d}_{\text{obs},j}^i \sim \mathcal{N}(\mathbf{d}_{\text{obs}}, \alpha_i \mathbf{C}_D).$$

8. Compute analysis step for every ensemble member:

$$\mathbf{m}_j^{i+1} = \mathbf{m}_j^i + \mathbf{C}_{\text{MD}}^i (\mathbf{C}_{\text{DD}}^i + \alpha_i \mathbf{C}_D)^{-1} (\mathbf{d}_{\text{obs},j}^i - \mathbf{d}_j^i).$$

9. Proceed to next iteration:

$$i = i + 1.$$

end (for).

2.2.1.2 Localization

Several authors report the need to use some localization technique when the assimilation is performed in large-scale models and using a limited ensemble size (e.g. Chen and Oliver (2010, 2016), Emerick (2016, 2018), Silva et al. (2017), Ranazzi and Sampaio (2018), Soares, Maschio and Schiozer (2018)). One widely method used in

the history matching apply the localization directly on the Kalman Gain matrix ($\mathbf{K} = \mathbf{C}_{MD}^i (\mathbf{C}_{DD}^i + \alpha_i \mathbf{C}_D)^{-1}$) using the Schur (elementwise) product, thus, the analysis equation becomes:

$$\mathbf{m}_j^{i+1} = \mathbf{m}_j^i + \boldsymbol{\rho} \circ \left[\mathbf{C}_{MD}^i (\mathbf{C}_{DD}^i + \alpha_i \mathbf{C}_D)^{-1} \right] (\mathbf{d}_{obs,j}^i - \mathbf{d}_j^i), \quad (45)$$

where $\boldsymbol{\rho}$ is the localization matrix and \circ represent the Schur product.

2.2.2 Posterior Data Matching

The discrepancy between the simulated and observed data is measured using the same objective function of the inflation factor definition (Eq. 35), that is, the norm between the observed and simulated production data weighted by the covariance of the measurement errors inverse.

2.2.3 Posterior Updated Models

The impact of the ensemble size in the uncertainty reduction also can be analyzed through the normalized variance (NV) and sum of normalized variance (SNV), that is, the relation between the posterior and prior model parameters ensemble variance (OLIVER; REYNOLDS; LIU, 2008; SOARES; MASCHIO; SCHIOZER, 2018; EMERICK, 2018). The normalized variance of a parameter can be determined as:

$$NV = \frac{\sigma_{posterior}^2}{\sigma_{prior}^2}, \quad (46)$$

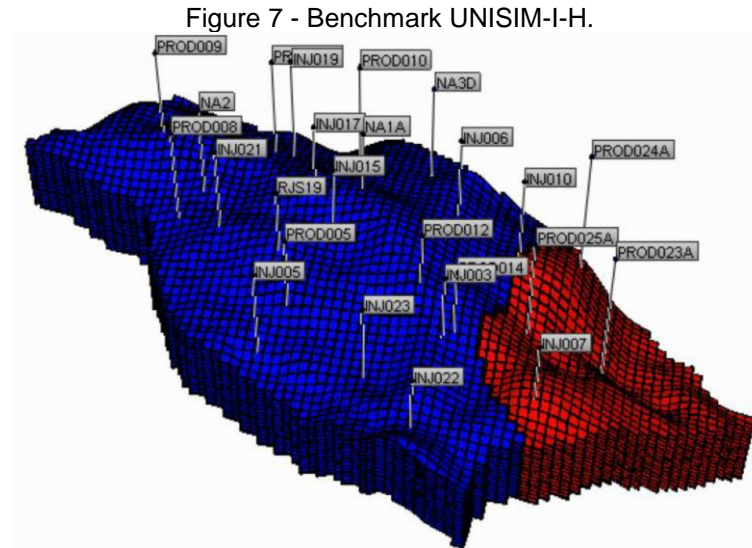
and the sum of normalized variance of a parameter set p containing a total of s parameters can be defined as:

$$SNV_p = \frac{\sum_{s=1}^{N_p} (\sigma_{posterior,s}^2 / \sigma_{prior,s}^2)}{N_p}, \quad (47)$$

2.3 Case Study

To evaluate the ensemble size influence on the adaptive ES-MDA history matching, we applied the methodology in the benchmark UNISIM-I-H for history

matching applications (MASCHIO et al., 2015). Avansi and Schiozer (2015) detail the construction of the benchmark. The black-oil reservoir model has 38466 active cells with one main fault that split the reservoir into two regions. The production history is composed of 11 years (4018 days) of 14 producer wells and 11 injector wells (oil and water production rate, gas-oil ratio, water injection rate and bottom-hole pressure). Figure 7 shows the reservoir model with the two sectors and the wells position.



There are about two hundred thousand uncertain parameters in the benchmark. The uncertain parameters are porosity, net-to-gross ratio, log-permeability in the three orthogonal directions (the log-permeability is used instead of permeability in order to represent the uncertainty as normal distribution), water-oil contact at the east sector, rock compressibility, vertical permeability multiplier; Corey exponent and maximum water relative permeability used to model the water relative permeability curve using Corey function. Table 1 shows the measurement errors used to create the covariance of the measurement errors matrix (C_D) in this case study. An important thing to point out is, if there is any zero value in a measurement type (like water production rate, for example), it is necessary to define a minimum error to keep the data as random variable.

Table 1 - Measurement errors.

Measurement Type	Measurement error
Oil production rate	10% (minimum of 1 m ³ /d)
Water production rate	15% (minimum of 1 m ³ /d min)
Gas-oil Ratio	20% (minimum of 10 m ³ /d min)
Water injection rate	05% (minimum of 1 m ³ /d min)
Bottom-hole pressure	5 kgf/cm ²

The localization matrix was built by performing distance-based localization using the well-known Gaspari and Cohn correlation (GASPARI; COHN, 1999). The influence area was defined as a circle (equal in x and y directions) with critical length equal to 2000 meters for all wells and data types. The iteration parameters used in this study were $\alpha_{\max} = 1000$, $a = 0.25$ and $i_{\max} = 15$, the influence was investigated by varying the ensemble size with minimum size equal to 100 members and maximum size equal to 500 members, with an increment equal to 100 members ($N_e = [100, 200, \dots, 500]$). The initial ensemble was created combining the information provided in the benchmark data (prior realizations of the petrophysical properties and probability density functions of the scalar properties). Table 2 shows the benchmark wells and field controls used during the 30 years (10957 days) forecast production period.

Table 2 – Forecast period controls.

	Control	Value	Action
Producer wells controls	Oil production rate	max 2000 m ³ /d min 20 m ³ /d	- Shutin
	Bottom-hole pressure	min 190 kgf/cm ²	-
	Watercut	max 0.9	Shutin
	Gas-oil rate	max 200	Shutin
Injector wells controls	Water injection rate	max 5000 m ³ /d	-
	Bottom-hole pressure	max 350 kgf/cm ²	-
Field controls	Liquid production rate	max 15500 m ³ /d	-
	Water production rate	max 13950 m ³ /d	-
	Oil production rate	max 15500 m ³ /d	-
	Water injection rate	max 21700 m ³ /d	-

2.4 Results and Discussion

Analyzing the discrepancy between the simulated and measured data through the averaged normalized objective function (\bar{O}_{N_d}) and the standard deviation of the normalized objective function (std $O_{N_d,j}$) of the prior and posterior ensembles (Table 3), it is possible to verify a similar and significant reduction in the objective function values for all cases. This similarity also can be verified by analyzing the evolution of the iterations of the normalized objective function $\bar{O}_{N_d}^i$ (Figure 8) and the inflation factor α_i (Figure 9) for different ensemble sizes, where both parameters presented similar behavior over the iterations regardless of the ensemble size. In addition, in Table 3 it is possible to verify that all cases required a similar number of iterations to complete the algorithm. This shows that the ensemble size has no influence on the number of iterations and on the selected inflation factors required to perform the adaptive methodology.

Table 3 - Prior and posterior objective function values (mean \pm standard deviation), required number of iterations and the total required simulation runs (including the posterior ensemble) for different ensemble sizes.

	$N_e = 100$	$N_e = 200$	$N_e = 300$	$N_e = 400$	$N_e = 500$
Prior	984.53 \pm 607.19	977.61 \pm 609.33	964.30 \pm 596.98	998.49 \pm 702.21	977.27 \pm 621.22
Posterior	5.18 \pm 2.64	4.12 \pm 1.33	3.17 \pm 2.05	4.14 \pm 3.49	4.32 \pm 3.43
N_i	8	8	9	8	8
Simul. Runs	900	1800	3000	3600	4500

Figure 8 - Averaged objective function evolution over the iterations for different ensemble sizes.

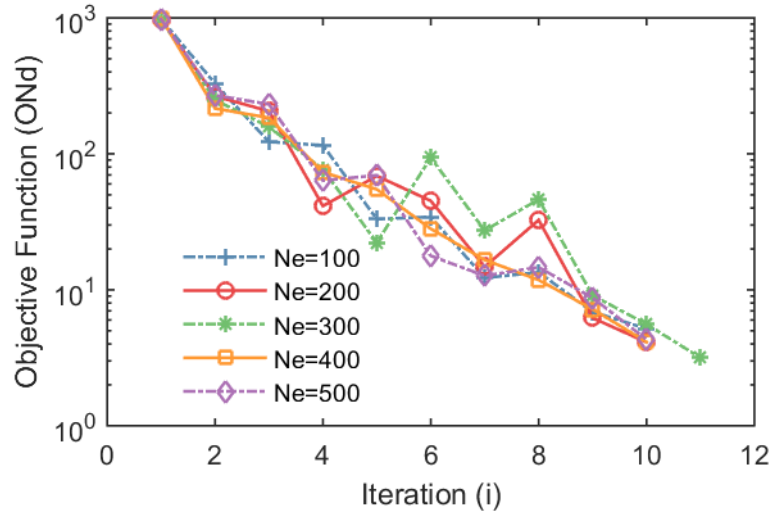
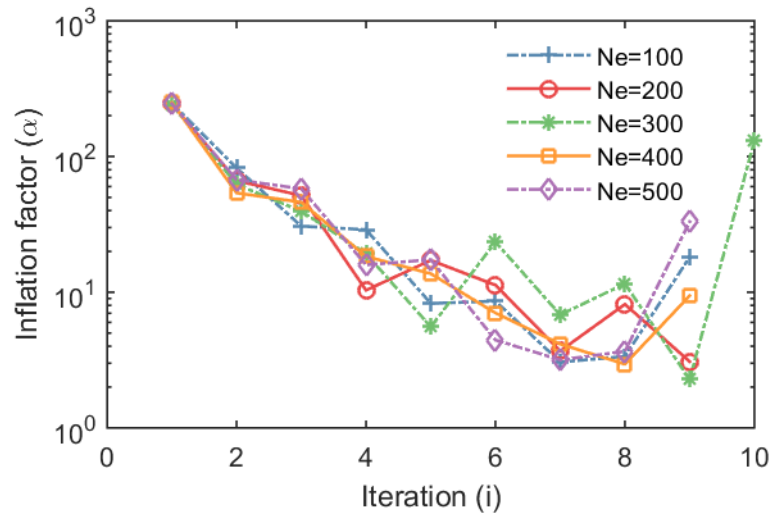


Figure 9 - Inflation factor evolution over the iterations for different ensemble sizes.



The matching between the observed and simulated data can also be verified by analyzing the well time series before and after the application of the adaptive ES-MDA (Figure 10 and Figure 11) for the case with ensemble size equal to 300. In the time series plots, the gray lines represent the prior ensemble, black lines represent the posterior ensemble and the red dots represent the observed data. Figure 10 shows the oil production rate (Figure 10 a,b), water rate (Figure 10 c,d) and bottom-hole pressure (BHP) (Figure 10 e,f) of two producer wells (NA3D and PROD023A). Figure 11 shows the water injection rate (Figure 11 a,b) and bottom-hole pressure (BHP) (Figure 11 c,d)

of two injector wells (INJ010 and INJ022). It is possible to verify an improvement at the posterior ensemble results for all wells and parameters analyzed due the adaptive methodology.

Figure 10 - Well time series of (a) NA3D Oil Rate, (b) PROD023A Oil Rate, (c) NA3D Water Rate, (d) PROD023A Water Rate, (e) NA3D Bottom-hole Pressure, (f) PROD023A Bottom-hole Pressure.

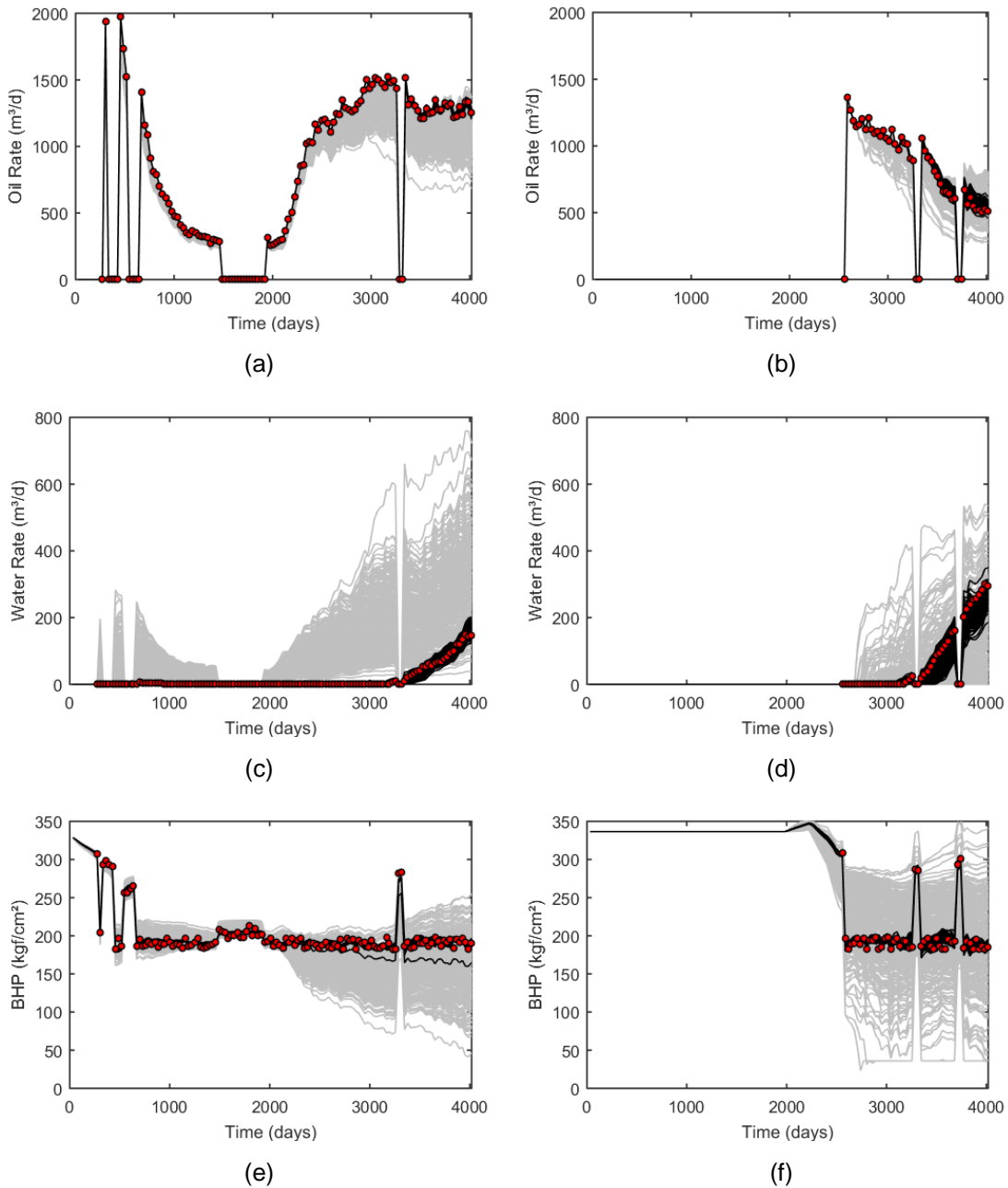
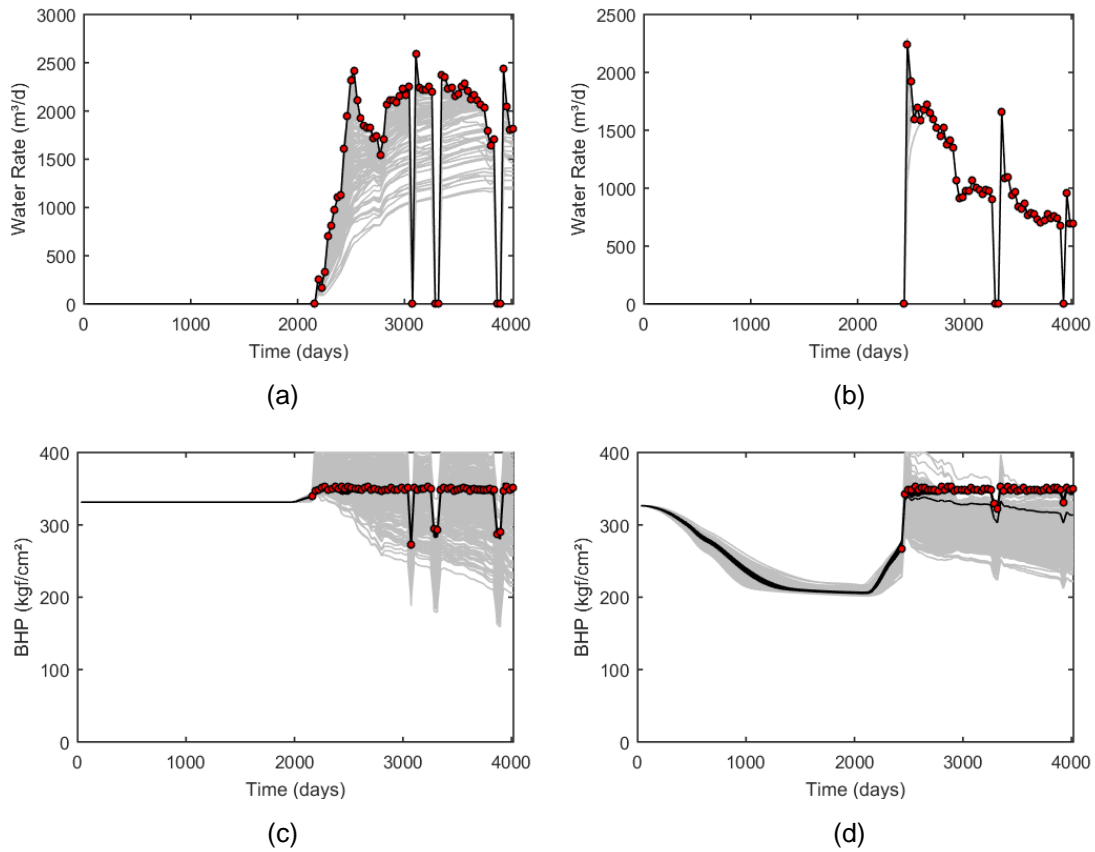
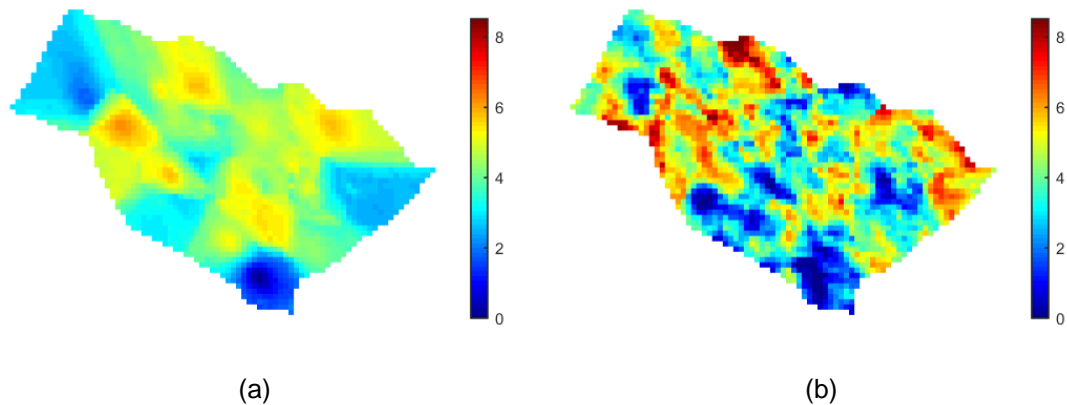
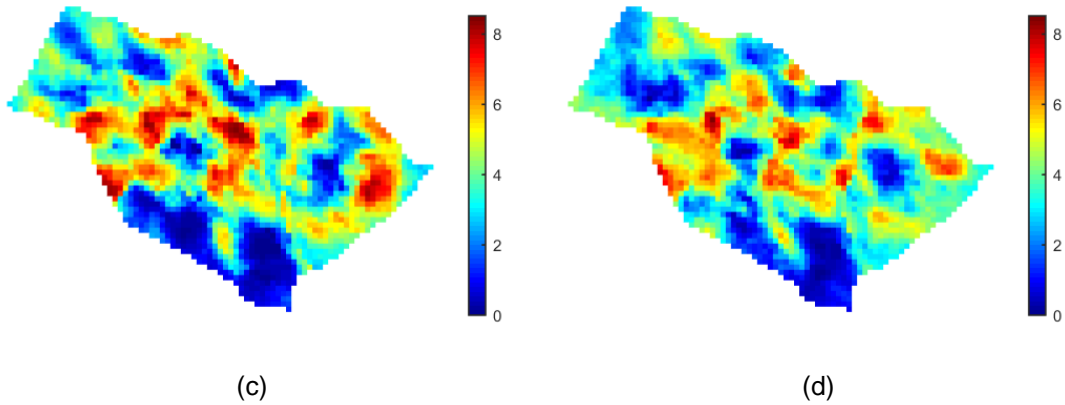


Figure 11 - Time series of injector well INJ010 and injector well INJ022.



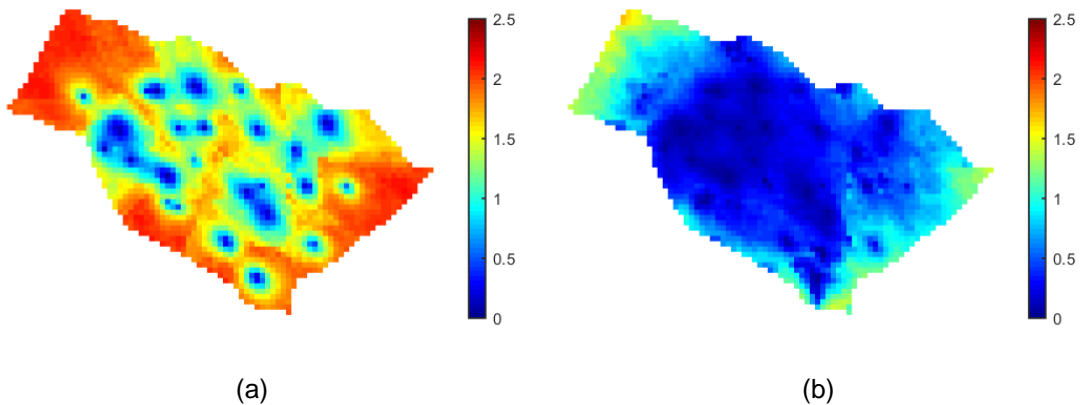
The update of the uncertain parameters after the matching is an important feature to be analyzed in order to preserve the prior reservoir characteristics as much as possible. Figure 12 shows the ensemble mean of the log-permeability in the i -direction (mean $\ln(k_x)$) for the prior and posterior models. It is possible to verify lower roughness and lesser extreme values (minimum and maximum $\ln(k_x)$ values) as the ensemble size increases.

Figure 12 - First layer mean log-permeability in i -direction a before (prior) and after (posterior) the history matching for ensemble size equal to (b) 100, (c) 300, (d) 500.



The ensemble size also influences the posterior log-permeability standard deviation in i-direction ($\text{std} \ln(k_x)$). The impact of the ensemble size in the uncertainty reduction also can be analyzed through the sum of normalized variance (SNV), that is, the relation between the posterior and prior model parameters ensemble variance (OLIVER; REYNOLDS; LIU, 2008; SOARES; MASCHIO; SCHIOZER, 2018; EMERICK, 2018). Table 4 shows the SNV of different uncertain model parameters for different ensemble sizes after the matching. Analyzing Figure 13 and Table 4, it is possible to verify smaller uncertainty reduction in the posterior ensemble as the ensemble size increases. It can be explained by the fact that analysis is contained in the space spanned by the initial ensemble (EVENSEN, 2007). Thus, the addition of more ensemble members increases the space spanned by the ensemble, improving the representation of the covariances C_{MD} and C_{DD} (that are estimated around the ensemble mean). The errors due the limited ensemble size will decrease proportional to $1/\sqrt{N_e}$ (EVENSEN, 2003).

Figure 13 - First layer log-permeability standard deviation in i-direction a before (prior) and after (posterior) the history matching for ensemble size equal to (b) 100, (c) 300, (d) 500



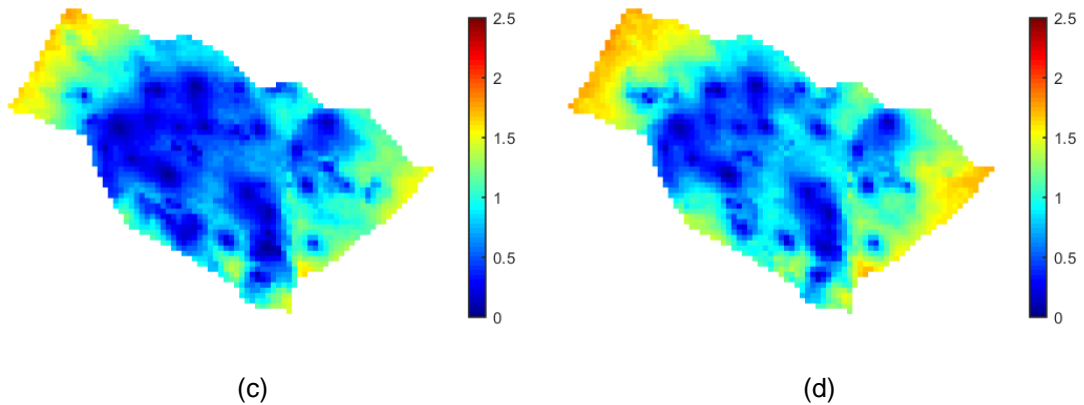
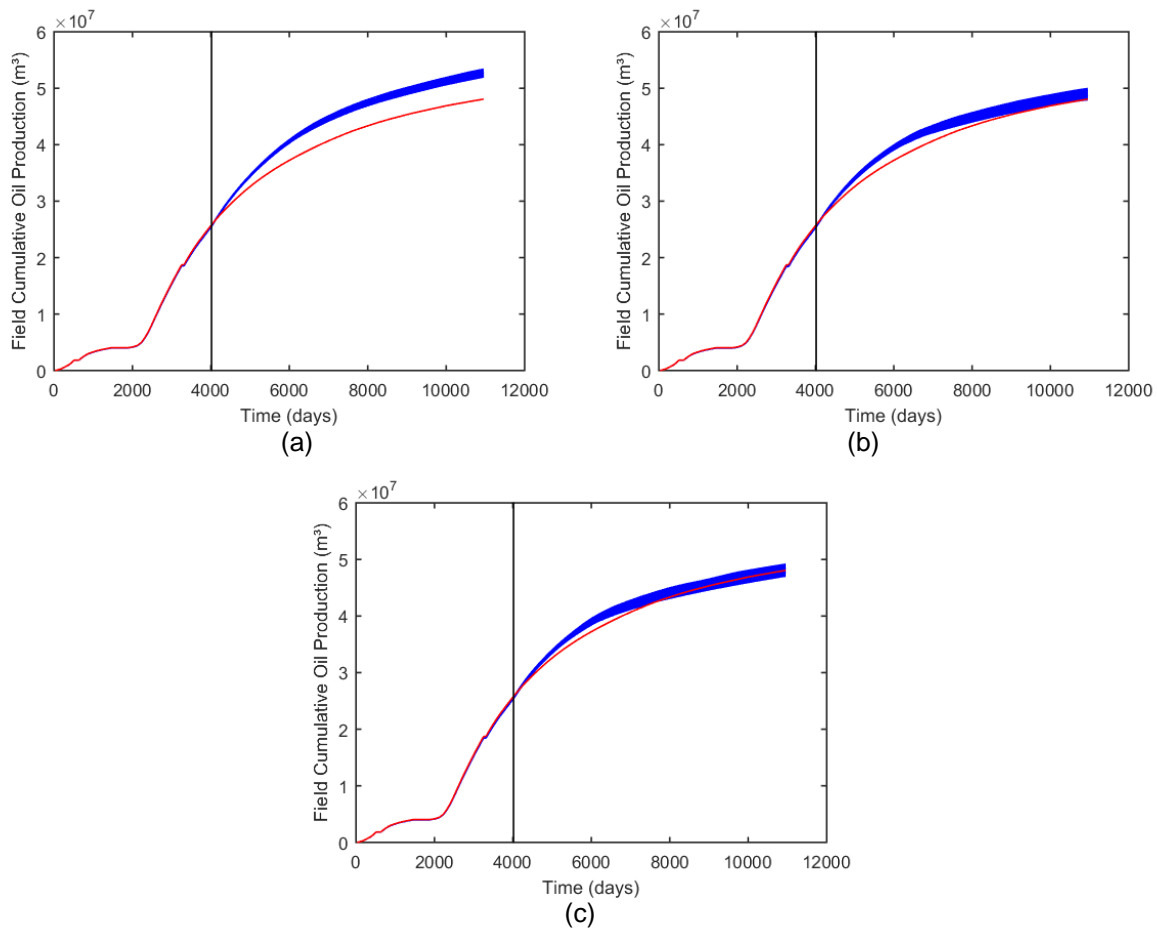


Table 4 - Sum of normalized variance for different ensemble sizes.

Parameter	$N_e = 100$	$N_e = 200$	$N_e = 300$	$N_e = 400$	$N_e = 500$
Porosity	0.3166	0.4308	0.5116	0.5675	0.6120
Net-to-gross	0.3528	0.4836	0.5680	0.6329	0.6821
Log-permeability (i)	0.3205	0.4340	0.5136	0.5712	0.6137
Log-permeability (j)	0.3208	0.4344	0.5140	0.5715	0.6139
Log-permeability (k)	0.2845	0.3924	0.4668	0.5249	0.5644
Water-oil contact	0.4852	0.5363	0.5488	0.6249	0.6858
Rock compressibility	0.0007	0.0104	0.0264	0.0381	0.0570
Vert. Perm. Multiplier	0.0015	0.0103	0.0226	0.0302	0.0448
Max. water Rel. Perm.	0.0011	0.0058	0.0202	0.0260	0.0422
Corey exponent	0.0011	0.0038	0.0129	0.0184	0.0242

Analyzing the forecast production period of 30 years, it is possible to verify the ensemble influence in the forecast period. Figure 14 shows the Field Cumulative Oil Production for different ensemble sizes, where the blue lines represent the posterior ensemble response, the red line represents the reference case (UNISIM-I-R) production response and the black vertical line represents the start of the forecast period (11 years). It is possible to verify that smaller ensemble sizes (Figure 14 a for $N_e = 100$ and Figure 14 b for $N_e = 300$) presented worse results in comparison to the higher ensemble size (Figure 14 c for $N_e = 500$).

Figure 14 - Forecast period field cumulative oil production for ensemble size equal to (a) 100, (b) 300, (c) 500.



2.5 Conclusion

This work investigated the ensemble size influence on the use of an adaptive ES-MDA for history matching, where the algorithm defines both the number of iterations and the inflation factors for each iteration. From the obtained results, the objective function and the inflation factor evolution over the iterations presented similar behavior, regardless of the ensemble size. Thus, it is possible to conclude that ensemble size definition did not influence in the required number of iterations to perform the algorithm or in the inflation factor selection in the adaptive scheme. The ensemble size mainly affects the update of the uncertain model parameters. It is possible to verify that smaller ensemble sizes (with lower computational cost required to perform the algorithm) resulted in high roughness and extreme updated parameters in the ensemble mean values and a higher uncertainty reduction in the posterior ensemble (analyzing both standard deviation and the SNV). The higher variance reduction may result in a poor uncertainty assessment of the production forecast

period, as can be seen in the analysis of the forecast production period. It is important to point out the fact that the ensemble size impact in the posterior ensemble was already verified in the literature (e.g. Soares, Maschio and Schiozer (2018)).

Regardless the updated models and the uncertainty assessment, the data matching objective function presented a good reduction for all ensemble sizes. This shows the ability of the adaptive ES-MDA to keep iterating until the algorithm reaches good data matchings, avoiding the explicit selection of the inflation factors. Thus, it is possible to define the importance of the correct selection of the ensemble size according to the available computational power, being an important feature the necessity of establish a balance between a good uncertainty assessment and the desired computation effort required to perform the algorithm.

2.6 Acknowledgements

The authors would like to thank the Polytechnic School of the University of São Paulo, CAPES (Coordination for the Improvement of Higher Education Personnel), FAPESP (São Paulo Research Foundation) and LASG (Laboratory of Petroleum Reservoir Simulation and Management) for supporting this research and study development, and CMG (Computer Modelling Group Ltd.) for providing the reservoir simulator licenses used in this study. The authors also would like to thank the UNISIM group for providing the UNISIM benchmark data, including the forecast period of the reference model. The authors are grateful for the valuable feedback and contribution from the anonymous reviewers.

CHAPTER 3 - INFLUENCE OF THE KALMAN GAIN LOCALIZATION IN ADAPTIVE ENSEMBLE SMOOTHER HISTORY MATCHING

Abstract

In reservoir engineering, history matching is the technique of conditioning a reservoir simulation model to the available production data. The reservoir properties have uncertainties which lead to discrepancies between the observed data and the reservoir simulator response, making history matching an indispensable tool in the petroleum industry. The standard Ensemble Smoother with Multiple Data Assimilation (ES-MDA) application has become popular in history matching problems. However, in the standard methodology, the number of iterations must be previously defined by the user, what makes it a determinant parameter in the ES-MDA results. One way to solve this problem is to perform adaptive algorithms: these algorithms keep iterating until they reach desirable matchings with the real data. Furthermore, to apply this method in large-scale reservoirs, it is necessary to use some localization technique to prevent spurious updates and high uncertainty reduction after the ES-MDA is applied. This work evaluates the influence of the distance-based Kalman Gain localization in an adaptive Ensemble Smoother, by applying the mentioned methodology in a large-scale synthetic reservoir model. The experiments showed a connection between the localization parameters and the number of iterations required by the adaptive algorithm. Moreover, the results presented significant reduction in the production data mismatch, regardless the localization, being the mismatch of the prior and posterior models an important parameter to determine the history matching quality.

3.1 Introduction

In the construction of a reservoir simulation model, many required properties have associated uncertainties due to their acquisition methods, resulting in a discrepancy between the simulated and observed data. The main purpose of the history matching process is re-evaluate the reservoir properties that have uncertainties in order to reproduce the behavior of observed data. With the technological advance of the history matching methods, an important feature of a good matching is to preserve the geological realism and quantify forecast uncertainty (ZHANG; OLIVER, 2011). In addition, history matching is generally an ill-posed inverse problem, which reinforces

the idea of using a method that quantifies the uncertainty, improving the reliability of reservoir performance prediction.

A set of methods that have been used in the history matching are the so-called “Ensemble-Methods”, where an ensemble of models are used to represent the parameters and forecast uncertainties. Some publications discuss the efficiency and recent progress in history matching (AANONSEN et al., 2009; OLIVER; CHEN, 2011; RWECHUNGURA; DADASHPOUR; KLEPPE, 2011). A widely used method is the Ensemble Kalman Filter (EnKF) (EVENSEN, 1994, 2003), a sequential data assimilation method. This concept means that the ensemble of model parameters is integrated forward in time (e.g., the reservoir simulator) and that in any period where observed data are available, the model ensemble is updated before the integration continues. The first application of the EnKF in a history matching problem was performed by Nævdal, Mannseth and Vefring (2002), where the near-well properties were updated. The EnKF is being widely studied since it is a suitable method to perform a continuous update of the reservoir models in a parameter-state estimation problem, by using 4D seismic data for real-time reservoir management. Some recent works present advances in the application of EnKF (HEIDARI et al., 2013; SHUAI et al., 2016), but their implementation in history matching has some practical issues. Some examples are the necessity to update the state variables (e.g., pressure and saturation of each grid block) and the simulation restarts at each assimilation step, making EnKF impractical for many cases. On the other hand, the Ensemble Smoother (ES) method (VAN LEEUWEN; EVENSEN, 1996) has gained attention recently in history matching. In ES, a single global update step containing all available observed data is performed in a parameter estimation problem. Skjervheim et al. (2011) applied for the first time the ES in a history matching problem, comparing its performance with EnKF. They concluded that, computationally, the ES is much faster than EnKF, it is easier to implement and provides an efficient ensemble-based method. The ES in its standard implementation has also some related issues, mainly due to the lack of the state updates at each assimilation step, presenting worse results in comparison to EnKF and requiring iterative methodologies to improve the ES efficiency (CHEN; OLIVER, 2012). Since then, many iterative ensemble smoothers have been developed. Chen and Oliver (2012) proposed a method based on the sequential ensemble randomized maximum likelihood method (EnRML) (GU; OLIVER, 2007), but with all the data assimilated simultaneously (batch-EnRML). In EnRML, the Gauss-Newton method is

used to minimize the difference between the simulated and observed data, using an average sensitivity matrix estimated from the ensemble. This method showed a significant reduction in the data mismatch, but the calculation of the sensitivity matrix is often unstable, resulting in a high number of iterations, sometimes with a computational cost greater than EnKF. Chen and Oliver (2013, 2014), proposed a variant of the EnRML using a Levenberg-Marquardt regularization scheme (LM-EnRML) in order to avoid the explicit calculation of the sensitivity matrix. Emerick and Reynolds (2013) define ES assimilation scheme as a method equivalent to a single Gauss-Newton iteration. Due to this, they propose a multiple data assimilation (MDA) method with the same formula of standard ES, but assimilating the same data multiple times. The ES-MDA uses an inflated covariance of the measurements errors to damp the changes in the model, in order to perform smaller corrections throughout each iteration. ES-MDA has been used in practical applications ever since (MAUCEC et al., 2016; BRESLAVICH et al., 2017). One of the disadvantages of the ES-MDA method is the need to determine, before the start of the algorithm, the number of iterations and the inflation factor of each iteration. The selection of these parameters must be correctly made in order to avoid overcorrections in the model parameters at each update step. These overcorrections can occur due to low damping in early Gauss-Newton iterations. Evensen (2018) showed that for a low number of iterations, better results can be achieved according to the selection of the inflation factor values at each iteration step. Le, Emerick and Reynolds (2016) presented an adaptive ES-MDA using the regularizing Levenberg-Marquardt algorithm (IGLESIAS; DAWSON, 2013) to automatically choose the inflation factors. These adaptive methodologies keep the algorithm iterating until it reaches low discrepancies in the data matching. This work compared the proposed methodology (ES-MDA-RLM) with the LM-EnRML, applying both in the three-phase 3D reservoir model called PUNQS3, showing better results with the less computational effort for ES-MDA-RLM application, but resulting in too high inflation factors at early iterations. These high early inflation factors may lead to an unfeasible number of iterations. In this context, Emerick (2016) proposed a simplified adaptive ES-MDA which the inflation factor is determined by a relationship with a normalized objective function that represents the discrepancy between the simulated and measured data.

In practical applications, the number of model parameters (around hundreds of thousands) is considerably higher than the ensemble size used in the assimilation

method. This fact may lead to the loss of variance of the model parameters ensemble (ensemble collapse) and a low-quality matching. One way to handle this is to apply some localization technique that limits the assimilation of each measurement according to their spatial position. There are several works that employ localization methods in ensemble-based assimilation techniques. Most of these works apply the localization by performing an element-wise multiplication (Schur product) between a localization matrix and the Kalman gain matrix of the assimilation scheme. Another localization procedure is to perform local analysis, where the analysis scheme is decomposed into local regions and each local analysis is performed only with the subset of the measurements within their respective region (EVENSEN, 2003; CHEN; OLIVER, 2016). Chen and Oliver (2016) analysed the Kalman gain localization and the Local Analysis (both localization methods) and concluded that both localization methods can give equivalent results if used with iterative methods (with the Local Analysis converging quickly when the number of data is higher in comparison to the ensemble size).

The matrix used in Kalman gain localization can be built from different approaches. Currently, the most used in reservoir history matching are distance-based and streamline-based localization. In distance-based localization, a correlation function is employed to calculate each element of the localization matrix. Emerick and Reynolds (2011a, 2011b) used the Gaspari and Cohn correlation (GASPARI; COHN, 1999) and proposed a methodology to determine the critical lengths of the correlation, based in the correlation lengths of the prior geological model and the drainage area of the wells. Silva et al. (2017) and Emerick (2018) performed a history matching where the critical length was defined by the authors as a circle of constant radius equal to 2000 meters, based on their previous experiences. Soares, Maschio and Schiozer (2018) proposed two approaches to estimate the critical length size, one that uses the influence area of each well in the producer-injector pair, and another that uses streamlines area to trace drainage ellipses in order to estimate the critical length in the distance-based localization. Chen and Oliver (2010, 2014) used a correlation function based on the ensemble size (FURRER; BENGTTSSON, 2007), where the bigger the ensemble size, the larger the influence area of the measurements. Watanabe and Datta-Gupta (2012) investigated the application of phase-streamlines to determine the influence area of the measurements in the Kalman gain localization, showing good results in reservoirs with high heterogeneity, where a simple distance-based cannot

represent the influence areas properly. However, streamline methodologies have a more difficult implementation, with the need to compute the streamline velocities along the reservoir model.

The case study of this paper is the UNISIM-I benchmark. Some studies have already applied the ES-MDA in UNISIM-I to perform history matching. Morosov and Schiozer (2017) and Silva et al. (2017) performed a closed-loop reservoir management (CLRM) in the case study for selection of production strategy UNISIM-I-D (GASPAR et al., 2015) using the standard ES-MDA methodology. Soares, Maschio and Schiozer (2018) applied the standard ES-MDA in UNISIM-I-H, using two different methods to define the critical length in Gaspari and Cohn correlation. Emerick (2018) tested a deterministic ES-MDA (DES-MDA) in UNISIM-I-H, where the measurements perturbation is avoided. This work aims to evaluate the influence of the critical length of Gaspari and Cohn correlation in an adaptive ES-MDA (EMERICK, 2016) plus Kalman gain localization, applying them in a large-scale synthetic reservoir model to verify the impact that the localization may cause in the adaptive assimilation scheme, filling the gap in the literature in regard to the impact of localization in adaptive algorithms applications.

3.2 Methodology

One of the main advantages of using an ensemble of model parameters in history matching problem is avoiding the explicit calculation of sensitivities. The ensemble uses the reservoir simulator response for each member to perform the assimilation, independently of the forward model system of equations. This work combines the adaptive Ensemble Smoother proposed by Emerick (2016) and the distance-based Kalman gain localization. The following sections describe the adaptive ES-MDA, the objective function that measures the data mismatch used to obtain the inflation factors of the ES-MDA and the application of the Kalman gain localization. In the methodology, we adopt the notation from Emerick (2016).

3.2.1 Adaptive ES-MDA

First, it is important to define the forward model and the inverse problem in the history matching. The perfect forward model, where the model errors are neglected (EVENSEN, 2018), can be defined as:

$$\mathbf{d} = g(\mathbf{m}) \quad (48)$$

where the forward operator g (in this case the reservoir simulator) relates the model parameters vector $\mathbf{m}_j \in \mathfrak{R}^{N_m}$ with the predicted data vector $\mathbf{d}_j \in \mathfrak{R}^{N_d}$, and, N_m and N_d are the number of model parameters and measurements, respectively. The history matching inverse problem is to estimate the model parameters that best represent the behavior of the available measurements of \mathbf{d} (\mathbf{d}_{obs}). Emerick and Reynolds (2013) define that ES is equivalent to a full Gauss-Newton update step. Therefore, the ES-MDA assimilates all the measurements multiple times, using an inflated covariance in the data noise, relating one iteration with a smaller Gauss-Newton update step. In the ES-MDA analysis step, each member j of model parameters vector ensemble is 'corrected' using the following analysis equation:

$$\mathbf{m}_j^{i+1} = \mathbf{m}_j^i + \mathbf{C}_{MD}^i (\mathbf{C}_{DD}^i + \alpha_i \mathbf{C}_D)^{-1} (\mathbf{d}_{obs,j}^i - \mathbf{d}_j^i) \quad (49)$$

for $j = (1, \dots, N_e)$, where N_e denotes the number of ensemble members (ensemble size), $\mathbf{C}_{MD}^i \in \mathfrak{R}^{N_m \times N_d}$ is the cross-covariance between the model parameters and predicted data, $\mathbf{C}_{DD}^i \in \mathfrak{R}^{N_d \times N_d}$ is the auto-covariance of the predicted data, α_i is the inflation factor that damp the iteration i , $\mathbf{C}_D \in \mathfrak{R}^{N_d \times N_d}$ is the covariance of the measurement errors. The forward step is where each ensemble member \mathbf{d}_j^i is estimated using the forward operator $\mathbf{d}_j^i = g(\mathbf{m}_j^i)$ for $j = (1, \dots, N_e)$. The term \mathbf{K} is the so-called Kalman Gain matrix:

$$\mathbf{K} = \mathbf{C}_{MD}^i (\mathbf{C}_{DD}^i + \alpha_i \mathbf{C}_D)^{-1} \quad (50)$$

In the analysis step, the measurements must be treated as random variables, adding to them a white Gaussian noise with covariance \mathbf{C}_D in order to prevent a too high reduction in the ensemble variance (BURGERS; VAN LEEUWEN; EVENSEN, 1998). In the ES-MDA, the errors are sampled using the following equation:

$$\mathbf{d}_{obs,j}^i = \mathbf{d}_{obs} + \sqrt{\alpha_i} \mathbf{C}_D^{1/2} \mathbf{z}_j, \quad (51)$$

where \mathbf{d}_{obs} is the vector containing the observed data (measurements), and \mathbf{z}_j is a Gaussian sample with $\mathbf{z}_j \sim \mathcal{N}(0, \mathbf{I}_{Nd})$. An important thing to point out is, assuming the observed data are uncorrelated (typical for production data), \mathbf{C}_D is a diagonal matrix the of form:

$$\mathbf{C}_D = \begin{bmatrix} \sigma_1^2 & 0 & \dots & 0 \\ 0 & \sigma_2^2 & & \vdots \\ \vdots & & \ddots & 0 \\ 0 & \dots & 0 & \sigma_{Nd}^2 \end{bmatrix}, \quad (52)$$

where σ represents the standard deviation of each measurement error. One of the characteristics of the ES-MDA is the fact that \mathbf{C}_{MD}^i and \mathbf{C}_{DD}^i are estimated around the ensemble mean. Then:

$$\mathbf{C}_{MD}^i = \frac{1}{Ne - 1} \sum_{j=1}^{Ne} (\mathbf{m}_j^i - \bar{\mathbf{m}}^i)(\mathbf{d}_j^i - \bar{\mathbf{d}}^i)^T, \quad (53)$$

and,

$$\mathbf{C}_{DD}^i = \frac{1}{Ne - 1} \sum_{j=1}^{Ne} (\mathbf{d}_j^i - \bar{\mathbf{d}}^i)(\mathbf{d}_j^i - \bar{\mathbf{d}}^i)^T, \quad (54)$$

where the overbars denote the ensemble mean:

$$\bar{\mathbf{m}}^i = \frac{1}{Ne} \sum_{j=1}^{Ne} \mathbf{m}_j^i, \quad (55)$$

and,

$$\bar{\mathbf{d}}^i = \frac{1}{Ne} \sum_{j=1}^{Ne} \mathbf{d}_j^i. \quad (56)$$

Emerick and Reynolds (2013) proved that for the ES-MDA to sample correctly the posterior model parameters in equivalence with the linear-Gaussian case, the inflation factors must be selected so that they obey the following condition over the N_i iterations:

$$\beta_i = \sum_{i=1}^{N_i} \frac{1}{\alpha_i} = 1. \quad (57)$$

In standard ES-MDA, the number of iterations and their inflation factors are defined previously by the user. Due to this, the ES-MDA cannot continue iterating if the algorithm does not provide a reasonable matching after N_i iterations. Therefore, it is necessary to restart the entire process, redefining the number of iterations and inflation factors. Emerick (2016) proposed an adaptive algorithm that directly relates the inflation factor to the data mismatch. This algorithm continues iterating until it reaches a desirable matching and reduces spurious correlations, since smaller step sizes (larger inflation factors) must be used in early iterations (LE; EMERICK; REYNOLDS, 2016).

In the adaptive ES-MDA, the inflation factor at each iteration is computed through the following equation:

$$\alpha_i = \min\{a\bar{O}_{Nd}^i, \alpha_{max}\}, \quad \text{with } a > 0 \quad (58)$$

where a is the coefficient that relates the inflation factor with an objective function that measures the discrepancy between the simulated and observed data \bar{O}_{Nd}^i , and α_{max} is the maximum inflation factor defined by the user. Before the analysis step at each iteration, the condition of Eq. 57 must be verified. If the condition $\beta_i > (1 - \alpha_{max}^{-1})$ is obtained or the maximum iteration number is reached ($N_i = N_{i,max}$), a new inflation factor must be calculated for β_i set equal to one, and the last iteration step is performed.

3.2.1.1 Ensemble representation and pseudo-inversion in the analysis

Dropping the iteration index in the analysis step, the ES-MDA can also be represented in matrix terms. We can define $\mathbf{M} \in \mathfrak{R}^{N_m \times N_e}$ and $\mathbf{D} \in \mathfrak{R}^{N_d \times N_e}$ the matrices holding the ensemble members \mathbf{m}_j and \mathbf{d}_j , respectively:

$$\mathbf{M} = [\mathbf{m}_1, \mathbf{m}_2, \dots, \mathbf{m}_{N_e}] \quad (59)$$

and,

$$\mathbf{D} = [\mathbf{d}_1, \mathbf{d}_2, \dots, \mathbf{d}_{N_e}] \quad (60)$$

According to Evensen (2004), the ensemble perturbation matrix can be represented as:

$$\mathbf{M}' = \mathbf{M} - \overline{\mathbf{M}} = \mathbf{M} \cdot (\mathbf{I} - \mathbf{1}_{N_e}) \quad (61)$$

and,

$$\mathbf{D}' = \mathbf{D} - \overline{\mathbf{D}} = \mathbf{D} \cdot (\mathbf{I} - \mathbf{1}_{N_e}) \quad (62)$$

where the overbars denote the matrix containing the ensemble mean in each column and the term $\mathbf{1}_{N_e} \in \mathfrak{R}^{N_e \times N_e}$ is a matrix where each element is equal to $1/N_e$. Thus, both covariances \mathbf{C}_{MD} and \mathbf{C}_{DD} can be constructed as a function of the ensemble perturbation matrix:

$$\mathbf{C}_{MD} = \frac{\mathbf{M}'(\mathbf{D}')^T}{N_e - 1} \quad (63)$$

and,

$$\mathbf{C}_{DD} = \frac{\mathbf{D}'(\mathbf{D}')^T}{N_e - 1} \quad (64)$$

Using the definitions of Eqs. (63) and (64), the analysis for each iteration i can be expressed in terms of ensemble perturbations as:

$$\mathbf{M}^{i+1} = \mathbf{M}^i + \mathbf{M}^i(\mathbf{D}'^i)^T \left[\mathbf{D}'^i(\mathbf{D}'^i)^T + (N_e - 1)\alpha_i \mathbf{C}_D \right]^{-1} (\mathbf{D}_{obs}^i - \mathbf{D}^i) \quad (65)$$

Dropping the iteration index again, the matrix $\mathbf{C} = \left[\mathbf{D}'^i(\mathbf{D}'^i)^T + (N_e - 1)\alpha_i \mathbf{C}_D \right]$ must be inverted, but it may be singular when the dimension of \mathbf{C} becomes large, being necessary compute the pseudo-inverse \mathbf{C}^+ of \mathbf{C} , since $\mathbf{C}^+ \equiv \mathbf{C}^{-1}$, when \mathbf{C} is full rank (EVENSEN, 2004). Evensen (2004) proposed a stable pseudo-inversion method called 'subspace inversion' for the case with a large number of measurements ($N_d \gg N_e$). In this method, a singular value decomposition (SVD) of \mathbf{D}' is used to compute the inverse in the N_e dimensional ensemble space (EVENSEN, 2004). According to Wang, Li and Reynolds (2010), very small singular values can result in errors, due to this, a truncated singular value decomposition (TSVD) is applied to estimate the pseudo-inverse during the procedure. Besides that, several authors report the need of scale the matrix \mathbf{C} before the inversion (EVENSEN, 2003; WANG; LI; REYNOLDS, 2010; EMERICK, 2016). This scale is needed for the reason that parameters of different magnitudes can have all respective singular values eliminated during the truncation.

An efficient way to perform this rescaling is using the measurement errors matrix in such a way that \mathbf{C} elements have the same variability (WANG; LI; REYNOLDS, 2010; EMERICK, 2016). The rescaling procedure used in this work was proposed by Emerick (2016), where the square root diagonal elements of \mathbf{C}_D were used to perform the rescaling before the inversion. Thus, the matrix \mathbf{C} after the scaling becomes:

$$\mathbf{C} = \mathbf{S}[\mathbf{S}^{-1}\mathbf{D}'(\mathbf{D}')^T\mathbf{S}^{-1} + (N_e - 1)\alpha\widehat{\mathbf{C}}_D]\mathbf{S} \quad (66)$$

where $\mathbf{S} \in \mathfrak{R}^{N_d \times N_d}$ is the matrix containing the square root of the diagonal elements of \mathbf{C}_D and $\widehat{\mathbf{C}}_D$ is the correlation matrix of the errors (EMERICK, 2016). When the observed data are uncorrelated, $\widehat{\mathbf{C}}_D$ is an identity matrix with size N_d .

The SVD of the matrix $\mathbf{S}^{-1}\mathbf{D}'$ is defined as:

$$\mathbf{S}^{-1}\mathbf{D}' = \mathbf{U}_0\mathbf{\Sigma}_0\mathbf{V}_0^T \quad (67)$$

where, $\mathbf{U}_0 \in \mathfrak{R}^{N_d \times N_d}$ and $\mathbf{V}_0 \in \mathfrak{R}^{N_e \times N_e}$ are orthogonal matrices containing the left and right singular vectors, respectively, and $\mathbf{\Sigma}_0 \in \mathfrak{R}^{N_d \times N_e}$ is the diagonal matrix containing the singular values λ ($\lambda_1 \geq \lambda_2 \geq \dots \geq \lambda_{N_d} > 0$) of the matrix $\mathbf{S}^{-1}\mathbf{D}'$. The TSVD retains only the N_r largest singular values, according to the following condition:

$$\frac{\sum_{i=1}^{N_r} \lambda_i}{\sum_{i=1}^{N_d} \lambda_i} \leq E \quad (68)$$

where E is the energy of the singular values retained. Thus:

$$\mathbf{S}^{-1}\mathbf{D}' \approx \mathbf{U}_r\mathbf{\Sigma}_r\mathbf{V}_r^T \quad (69)$$

where $\mathbf{U}_r \in \mathfrak{R}^{N_d \times N_r}$, $\mathbf{V}_r \in \mathfrak{R}^{N_r \times N_e}$ and $\mathbf{\Sigma}_r \in \mathfrak{R}^{N_r \times N_r}$. The pseudo-inverse of the matrix $\mathbf{S}^{-1}\mathbf{D}'$ is defined as:

$$(\mathbf{S}^{-1}\mathbf{D}')^+ \approx \mathbf{V}_r\mathbf{\Sigma}_r^+\mathbf{U}_r^T \quad (70)$$

where $\mathbf{\Sigma}_r^+$ is defined as $\text{diag}(\mathbf{\Sigma}_r^+) = (\lambda_1^{-1}, \lambda_2^{-1}, \dots, \lambda_{N_r}^{-1})$. This subspace inversion using the TSVD of $\mathbf{S}^{-1}\mathbf{D}'$ extract only the subspace consisting of the N_r dominant directions in \mathbf{U}_r (EVENSEN, 2004). Using the approximation, the matrix \mathbf{C} can be defined as:

$$\mathbf{C} \approx \mathbf{S}\mathbf{U}_r\mathbf{\Sigma}_r(\mathbf{I}_r + (N_e - 1)\alpha\mathbf{\Sigma}_r^+\mathbf{U}_r^T\widehat{\mathbf{C}}_D\mathbf{U}_r\mathbf{\Sigma}_r^{+T})\mathbf{\Sigma}_r^T\mathbf{U}_r^T\mathbf{S} \quad (71)$$

where $\mathbf{R} = (N_e - 1)\alpha\mathbf{\Sigma}_r^+\mathbf{U}_r^T\widehat{\mathbf{C}}_D\mathbf{U}_r\mathbf{\Sigma}_r^{+T}$ is a real-symmetric matrix. Applying SVD to \mathbf{R} ,

$$\mathbf{R} = \mathbf{Z}_r\mathbf{\Lambda}_r\mathbf{Z}_r^T \quad (72)$$

and applying this in Eq. (71), \mathbf{C} becomes:

$$\mathbf{C} \approx \mathbf{S} \mathbf{U}_r \Sigma_r \mathbf{Z}_r (\mathbf{I}_r + \mathbf{\Lambda}_r) \mathbf{Z}_r^T \Sigma_r^T \mathbf{U}_r^T \mathbf{S}. \quad (73)$$

Being $\Sigma_r^+ = \Sigma_r^{+T}$ and $\mathbf{S} = \mathbf{S}^T$, the pseudo-inverse of \mathbf{C} becomes:

$$\mathbf{C}^+ = (\mathbf{S}^{-1} \mathbf{U}_r \Sigma_r^+ \mathbf{Z}_r) (\mathbf{I}_r + \mathbf{\Lambda}_r)^{-1} (\mathbf{S}^{-1} \mathbf{U}_r \Sigma_r^+ \mathbf{Z}_r)^T. \quad (74)$$

3.2.2 Objective Functions

A very common way to measure this discrepancy is through the quadratic difference between the simulated and observed data, normalized by the measurement errors matrix, so that the errors have the same magnitude (SILVA et al., 2016; LE; EMERICK; REYNOLDS, 2016; EMERICK, 2016). The normalized objective function that represents the data-mismatch for each member j at each iteration is:

$$\mathbf{o}_{Nd,j}^i = \frac{1}{2N_d} (\mathbf{d}_j^i - \mathbf{d}_{obs})^T \mathbf{C}_D^{-1} (\mathbf{d}_j^i - \mathbf{d}_{obs}), \quad (75)$$

and the averaged objective function is defined by:

$$\bar{\mathbf{o}}_{Nd}^i = \frac{1}{N_e} \sum_{j=1}^{N_e} \mathbf{o}_{Nd,j}^i. \quad (76)$$

A way to verify the mismatch of the updated models is through an objective function similar to that used in the data matching (Eq. 76). Chen and Oliver (2016) define an objective function to measure the changes as:

$$\mathbf{O}_{Nm,j} = (\mathbf{m}_{pr,j} - \mathbf{m}_j)^T \mathbf{C}_M^{-1} (\mathbf{m}_{pr,j} - \mathbf{m}_j) \quad (77)$$

where \mathbf{m}_{pr} and \mathbf{m} denotes the prior and updated vector of model parameters, respectively, and $\mathbf{C}_M \in \mathfrak{R}^{N_m \times N_m}$ is the covariance of the prior model parameters. The number of parameters in large-scale problems is an issue that makes the construction of \mathbf{C}_M (in this case study specifically, \mathbf{C}_M would be a 192335×192335 matrix) and calculation of its inverse \mathbf{C}_M^{-1} (or pseudo-inverse \mathbf{C}_M^+) unfeasible. In this equation, the only function of \mathbf{C}_M^{-1} is scaling the deviations of each parameter. Thus, an approximation was performed, resulting in an equation similar to $\mathbf{O}_{Nd,j}$, that can be used to calculate the mismatch where the deviations are normalized:

$$\tilde{\sigma}_{N_m,j}^i = \frac{1}{N_m} \sum_{m=1}^{N_m} \left(\frac{\mathbf{m}_{m,j}^{pr} - \mathbf{m}_{m,j}^i}{\sigma_m^{pr}} \right)^2 \quad (78)$$

where σ_m^{pr} represents the standard deviation of a parameter m in the prior ensemble. Similar to this, the averaged objective function for the model mismatch becomes:

$$\tilde{\sigma}_{N_m}^i = \frac{1}{N_e} \sum_{j=1}^{N_e} \tilde{\sigma}_{N_m,j}^i \quad (79)$$

3.2.3 Kalman Gain Localization

In most of the practical large-scale reservoir history matching problems, the number of model parameters is much higher compared to the ensemble size ($N_m \gg N_e$). In standard assimilation applications, this fact can lead to spurious correlations and near ensemble collapse (high reduction in ensemble variance) in the updated model parameters. One way to reduce these effects is to apply a localization technique in the analysis scheme to increase the number of degrees of freedom (CHEN; OLIVER, 2016).

This work will apply the localization directly in the Kalman Gain matrix, where the localization is performed using the element-wise product (Schur product) between the localization matrix $\boldsymbol{\rho} \in \mathfrak{R}^{N_m \times N_d}$ and the Kalman Gain matrix:

$$\tilde{\mathbf{K}} = \boldsymbol{\rho} \circ \mathbf{K} \quad (80)$$

Then, the analysis scheme in the adaptive ensemble smoother can be performed using the same form than no-localization methodology:

$$\mathbf{m}_j^{i+1} = \mathbf{m}_j^i + \tilde{\mathbf{K}}(\mathbf{d}_{obs,j}^i - \mathbf{d}_j^i) \quad (81)$$

Each element of $\boldsymbol{\rho}$ is a number between 0 and 1 to weight the matrix \mathbf{K} based on the spatial positions of the model parameters and data:

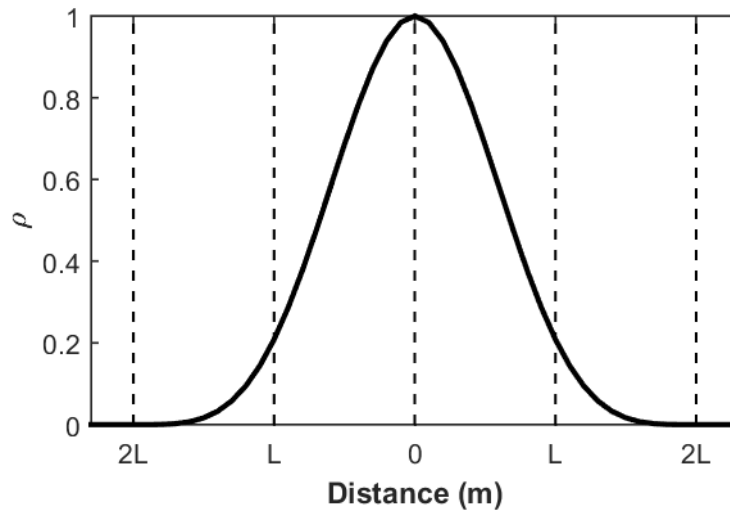
$$\boldsymbol{\rho} = \begin{bmatrix} \rho_{m_1,d_1} & \rho_{m_1,d_2} & \cdots & \rho_{m_1,d_{Nd}} \\ \rho_{m_2,d_1} & \rho_{m_2,d_2} & & \rho_{m_2,d_{Nd}} \\ \vdots & & \ddots & \vdots \\ \rho_{m_{N_m},d_1} & \rho_{m_{N_m},d_2} & \cdots & \rho_{m_{N_m},d_{Nd}} \end{bmatrix} \quad (82)$$

In distance-based localization, a correlation function is used to determine the values of ρ according to the distance between the model parameter and the data. One of the most used, is the correlation proposed by Gaspari and Cohn (1999):

$$\rho_{m,d} = \begin{cases} -\frac{1}{4}\left(\frac{z}{L}\right)^5 + \frac{1}{4}\left(\frac{z}{L}\right)^4 + \frac{5}{8}\left(\frac{z}{L}\right)^3 - \frac{5}{3}\left(\frac{z}{L}\right)^2 + 1, & 0 \leq z \leq L \\ \frac{1}{12}\left(\frac{z}{L}\right)^5 - \frac{1}{2}\left(\frac{z}{L}\right)^4 + \frac{5}{8}\left(\frac{z}{L}\right)^3 + \frac{5}{3}\left(\frac{z}{L}\right)^2 - 5\left(\frac{z}{L}\right) + 4 - \frac{2}{3}\left(\frac{L}{z}\right) & L \leq z \leq 2L \\ 0, & 2L \leq z \end{cases} \quad (83)$$

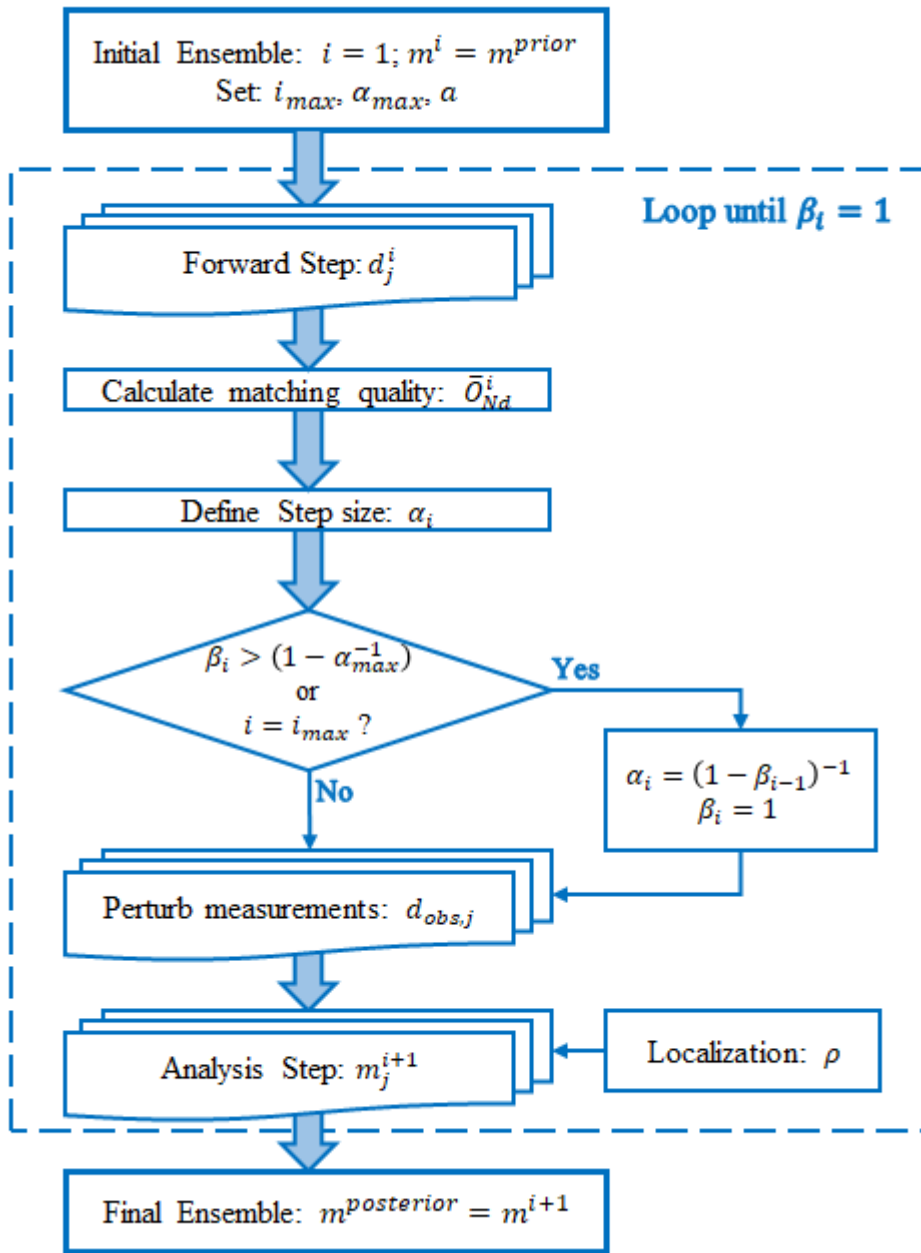
where z is the Euclidean distance between the location of model parameter m and the data d and L is the critical length. Figure 15 show the shape of Gaspari and Cohn correlation as a function of the critical length.

Figure 15 - Gaspari-Cohn correlation as a function of critical length.



In this work, the methodology will be tested by varying the critical lengths mentioned above, and their impact on the adaptive ES-MDA will be analyzed. Figure 16 illustrates the adopted workflow of the adaptive ES-MDA plus Kalman gain localization.

Figure 16 - Workflow of the adaptive ES-MDA plus Kalman gain localization.

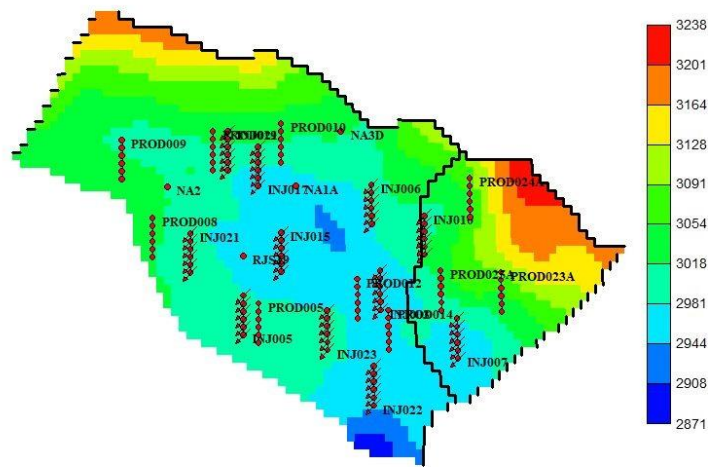


3.3 Case Study

The simulation model used in this work is the UNISIM-I-H benchmark for history matching (MASCHIO et al., 2015). The UNISIM-I synthetic reservoir model was built using public data from Namorado Field, a Brazilian offshore field in Campos Basin (AVANSI; SCHIOZER, 2015). This black oil reservoir model is composed of a corner point grid (81x58x20 cells), with 38466 active gridblocks and one main fault that separate the reservoir into two sectors. UNISIM-I-H contains 11 years of production

history of 14 producer wells and 11 injector wells, and the dataset is composed by monthly measurements of oil and water production rate, gas-oil ratio (GOR), water injection rate and bottom-hole pressure (BHP) of all wells. Measurements were obtained through the fine-scale UNISIM-I-R (326x234x157 cells) reference model and a random noise was added to the observed well data (MASCHIO et al., 2015). Figure 17 shows the position of the fault and the location of wells projected into the first layer grid top of the UNISIM-I-H.

Figure 17 - First layer grid top of UNISIM-I-H benchmark (wells projected).



The uncertainties of the case study can be separated into two categories: petrophysical properties (grid values) and global properties (scalar values). The prior petrophysical uncertainties set consists of equiprobable realizations containing porosity, net-to-gross ratio, and permeability in the three orthogonal directions. The global uncertainties are the water-oil contact at the east sector, rock compressibility, vertical permeability multiplier and two parameters related to the water relative permeability curve (Corey exponent and the maximum water relative permeability). The Corey function was used to model the water relative permeability curve. The uncertain properties were used according to the benchmark description (MASCHIO et al., 2015), the total number of data points is $N_d = 5552$ and the total number of model parameters is $N_m = 192335$.

In this history matching problem, the producer wells control is made by liquid rate and the injector wells control is made by the water injection rate. It is important to note that water injection rate is used as a measurement to be assimilated even when steered, since not always the controlled values can be satisfied during the simulation of the entire ensemble. As pointed before, the measurements in the analysis scheme

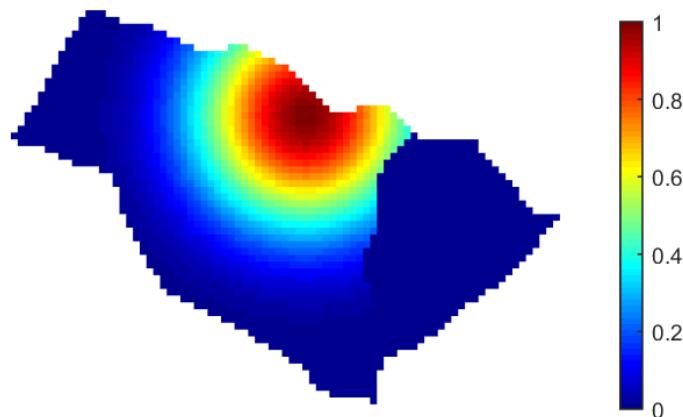
need to be treated as random variables. Table 1 shows the measurement errors used in this study to construct the measurement errors matrix C_D . It is important to point out the fact that parameters with values equal to zero (for example, oil and water rate) must have a minimum error to keep treating that parameter as random variable.

Table 5 - Measurement errors in data assimilation used to construct the measurement errors matrix.

Measurement Type	Measurement error
Oil production rate	10% (minimum of 1 m ³ /d)
Water production rate	15% (minimum of 1 m ³ /d min)
Gas-oil Ratio	20% (minimum of 10 m ³ /d min)
Water injection rate	05% (minimum of 1 m ³ /d min)
Bottom-hole pressure	5 kgf/cm ²

The adaptive ES-MDA were applied in the case study to assimilate the production data available using an ensemble size equal to $N_e = 200$ and the effect of Kalman Gain localization was analyzed varying the critical length (without localization, L varying from 1000 m to 3000 m). All cases use the following iteration parameters: $\alpha_{max} = 1000$, $a = 0.25$ and $N_{i,max} = 15$. In subspace inversion, 99% of the singular values energy was retained ($E = 0.99$). In the construction of the localization matrix for the petrophysical uncertainties, the $\rho_{m,d}$ were truncated to have only nonzero values, if the parameter and data were located in the same sector of the reservoir (being an implementation similar to the local analysis procedure). Regarding to the global uncertainties, only the water-oil contact of the east sector was restricted to assimilate just the data from their respective sector. Figure 18 shows an example of the localization matrix (ρ values) using this procedure.

Figure 18 - Values of ρ in the localization matrix for producer well NA3D and $L = 2000$ m.



3.4 Results of Assimilation of Production Data

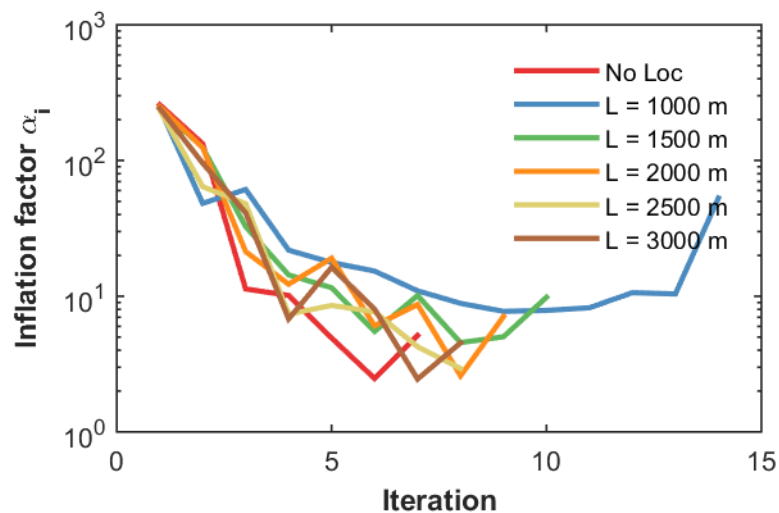
The history matching using the adaptive ES-MDA presented a reduction in the data mismatch objective function from 967.08 to 4.14 (for $L = 2500$ m) approximately. Table 2 shows the mean and standard deviation for O_{Nd} and \tilde{O}_{Nm} , for the prior and posterior model ensembles for each case after applying the methodology. The values for the data matching objective function show that the methodology provides a high reduction in the data mismatch, regardless of the critical distance value. Besides that, it is possible to verify an improvement due to the use of the localization, except for the case with the lowest critical length of the study ($L = 1000$ m).

Table 6 - Mismatch of data and model objective functions (mean \pm standard deviation).

L (m)	N_i	O_{Nd}	\tilde{O}_{Nm} (10^{-6})
Prior	-	967.0853 \pm 632.0824	-
1000	14	19.5446 \pm 20.3951	5.0764 \pm 0.3119
1500	10	4.6623 \pm 2.5942	7.1995 \pm 0.4037
2000	9	4.2966 \pm 3.1282	9.2001 \pm 0.4860
2500	8	4.1440 \pm 2.5013	10.5394 \pm 0.5571
3000	8	4.4740 \pm 2.0890	11.3698 \pm 0.5707
No localization	7	7.3220 \pm 0.2700	20.1602 \pm 1.1311

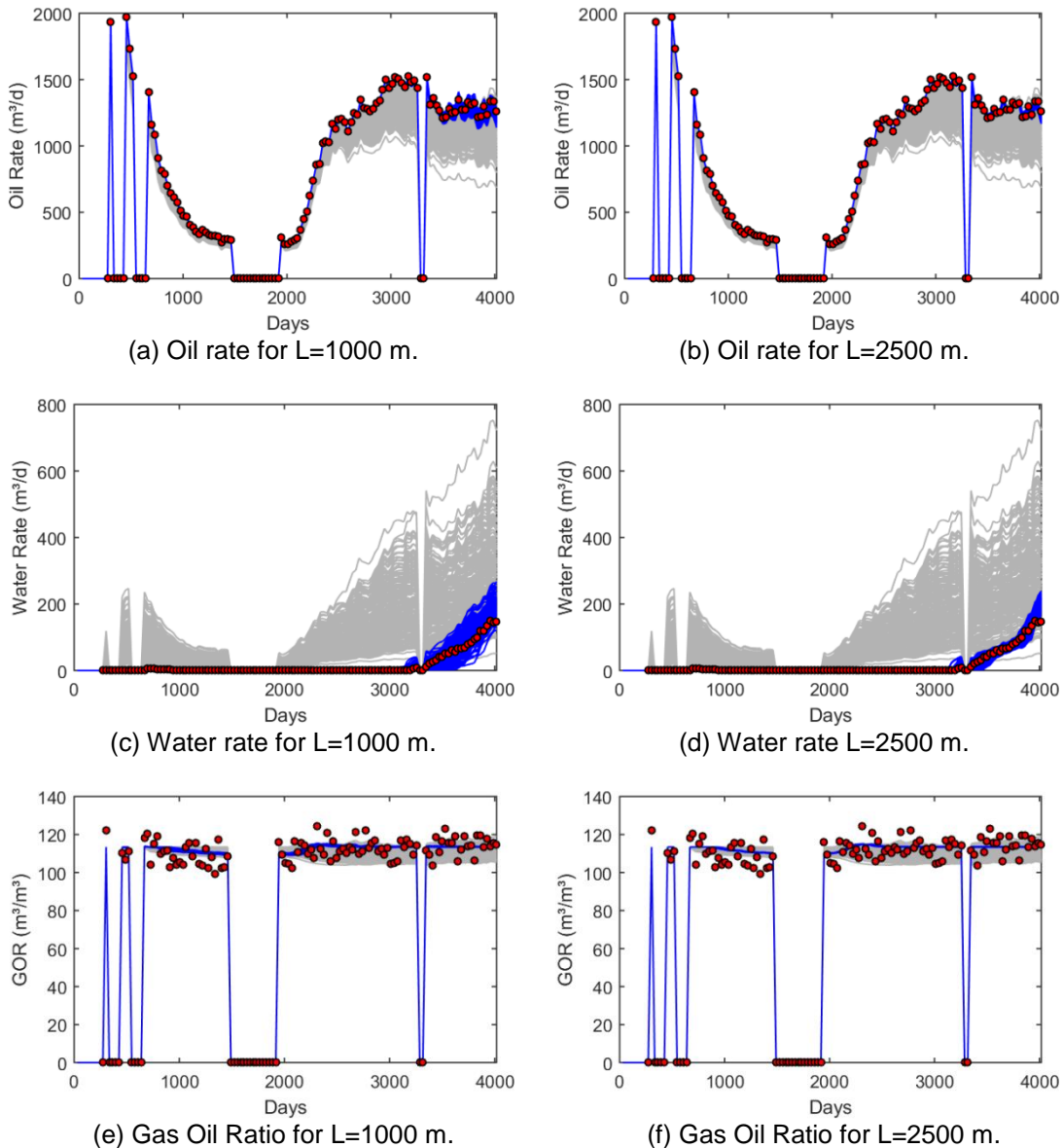
Analyzing the inflation factor evolution over the iterations (Figure 19), it is also possible to verify that the case mentioned above ($L = 1000$ m) took a high number of iterations to perform the algorithm, and even then, it presented worse results compared with the no localization case. One possible reason for this is the fact that very low critical length values greatly reduce the effective number (nonzero elements in the localization matrix) of model parameters to be assimilated.

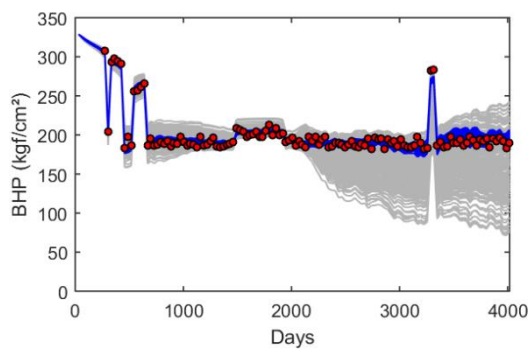
Figure 19 - Inflation factor evolution over iterations for different critical lengths.



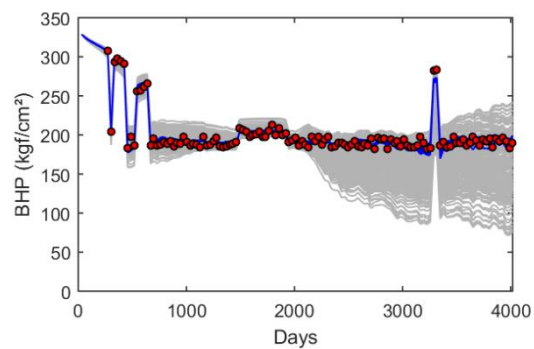
The effectiveness of the matching can also be verified through the well time series for the prior and posterior models parameters. Figure 20 to Figure 23 shows the time series of one producer and one injector well of each sector for the cases with worse and better \bar{O}_{Nd} values ($L = 1000$ m and 2500 m, respectively), where the gray lines represents the prior ensemble, blue lines represent the posterior ensemble and the red dots represent the history data. Both cases present satisfactory results, but it is clear to see an improved matching for the lowest \bar{O}_{Nd} case ($L = 2500$ m), especially in the water rate of the producer wells (Figure 20c,d, Figure 21c,d).

Figure 20 - Time series of producer well NA3D. The gray lines represent the prior ensemble and the blue lines represent the posterior ensemble, red dots are the measurements.



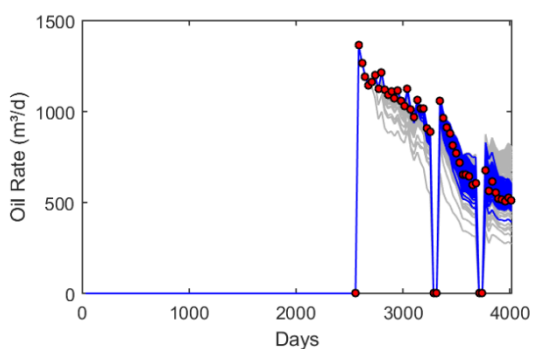


(g) Bottom-hole pressure for L=1000 m.

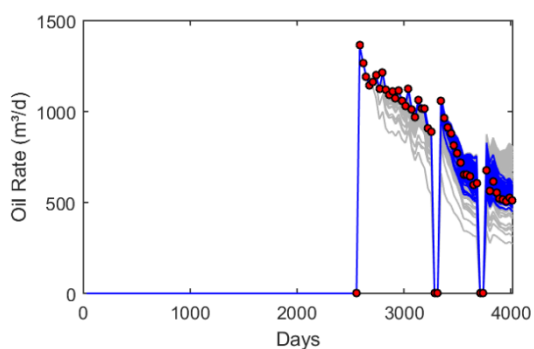


(h) Bottom-hole pressure for L=2500 m.

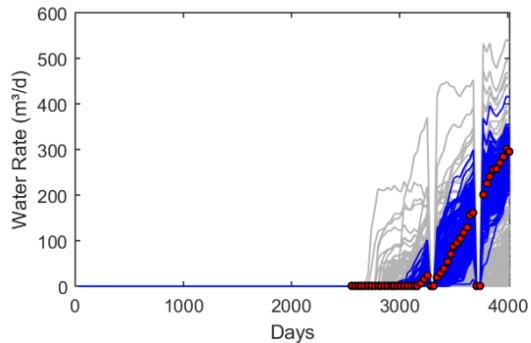
Figure 21 - Time series of producer well PROD023A. The gray lines represent the prior ensemble and the blue lines represent the posterior ensemble, red dots are the measurements.



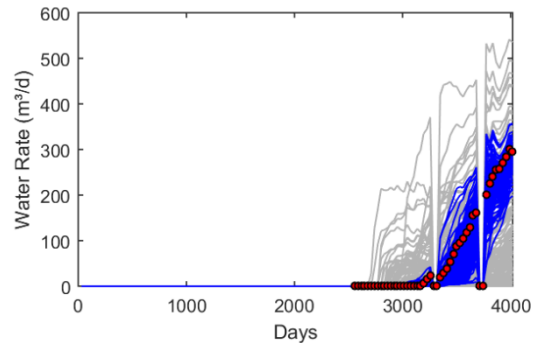
(a) Oil rate for L=1000 m.



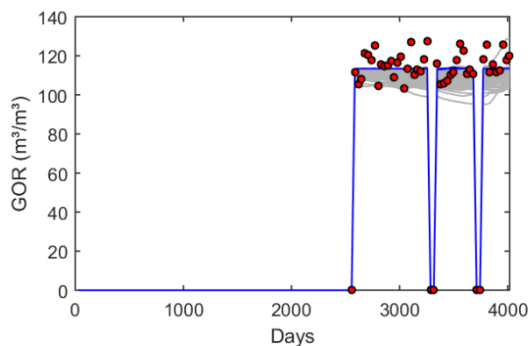
(b) Oil rate for L=2500 m.



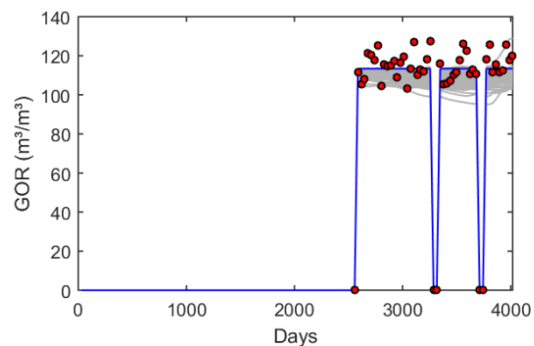
(c) Water rate for L=1000 m.



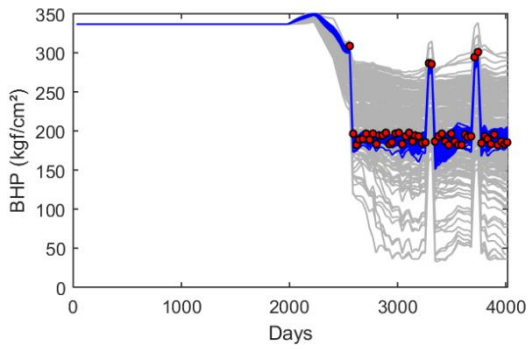
(d) Water rate L=2500 m.



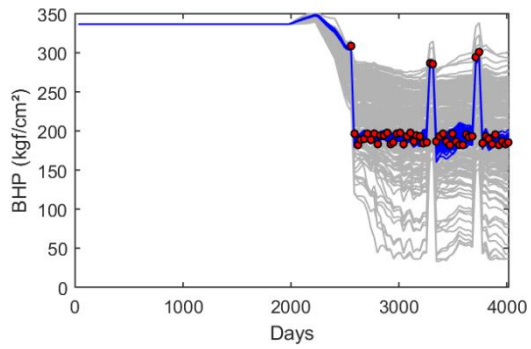
(e) Gas Oil Ratio for L=1000 m.



(f) Gas Oil Ratio for L=2500 m.

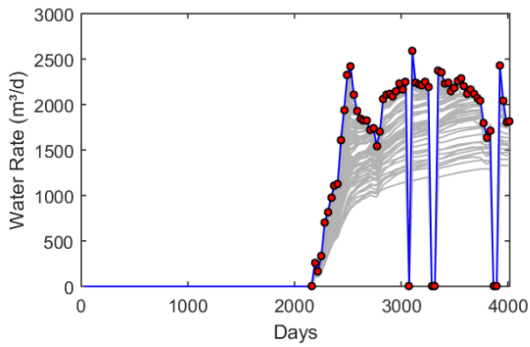


(g) Bottom-hole pressure for L=1000 m.

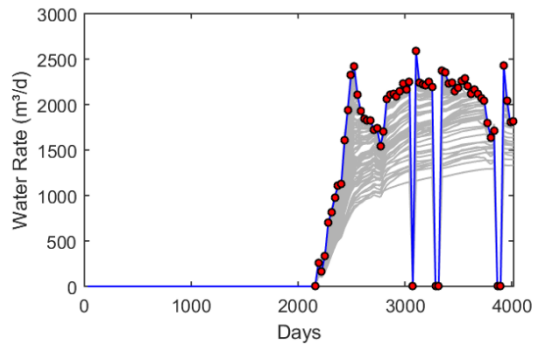


(h) Bottom-hole pressure for L=2500 m.

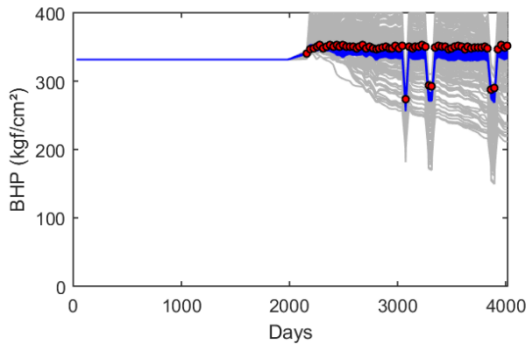
Figure 22 - Time series of water injector well INJ010. The gray lines represent the prior ensemble and the blue lines represent the posterior ensemble, red dots are the measurements.



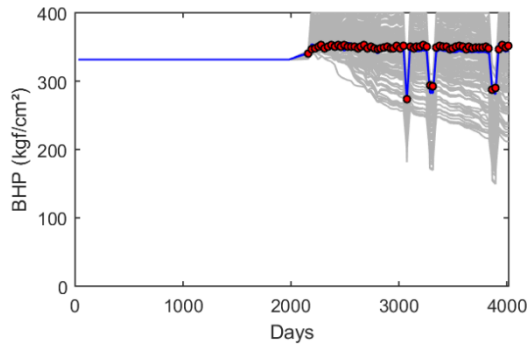
(a) Water rate for L=1000 m.



(b) Water rate L=2500 m.

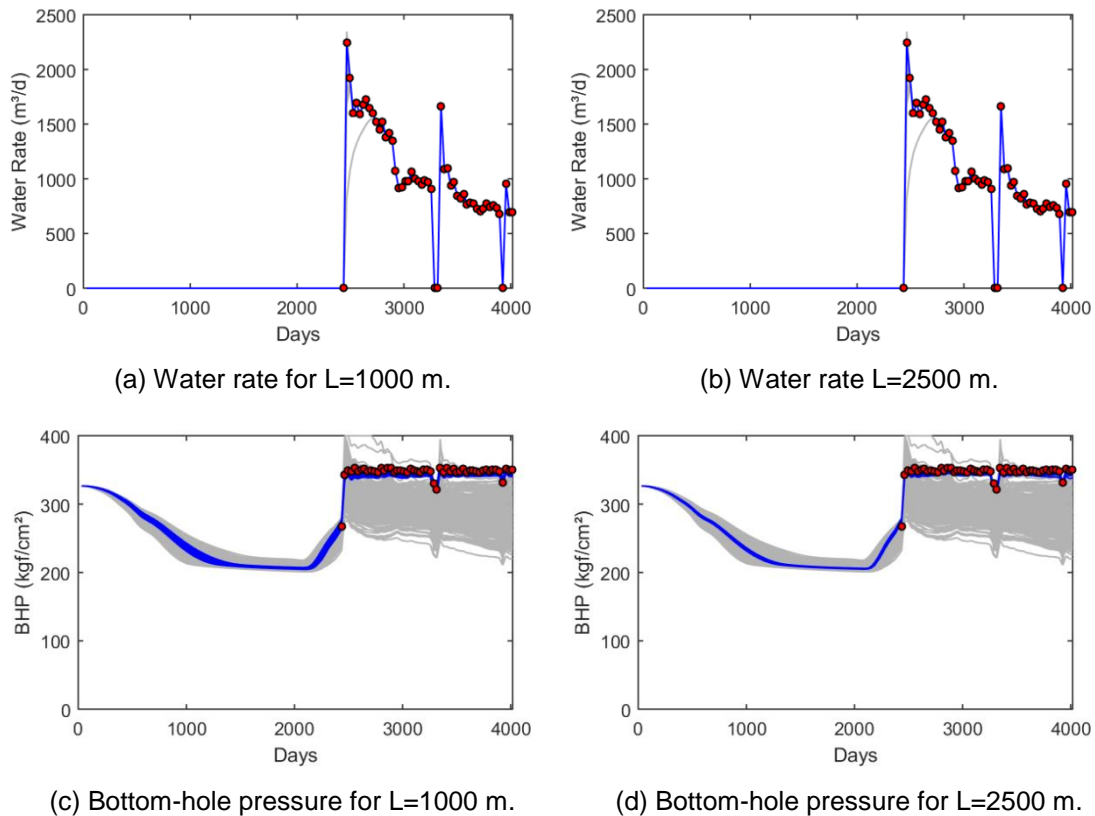


(c) Bottom-hole pressure for L=1000 m.



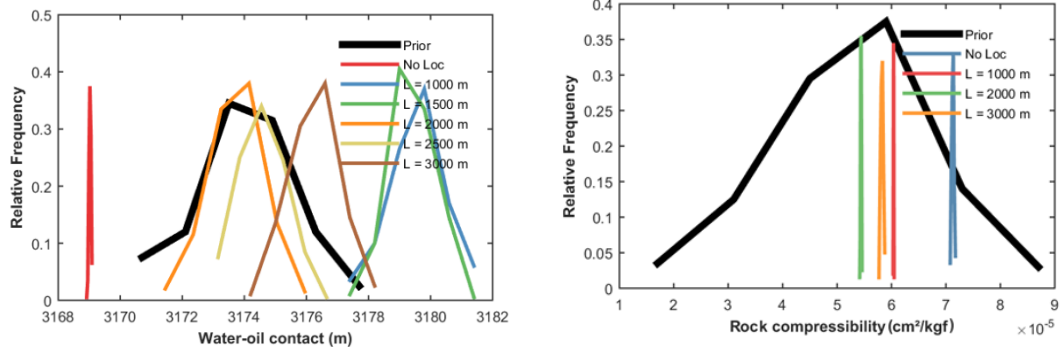
(d) Bottom-hole pressure for L=2500 m.

Figure 23 - Time series of water injector well INJ022. The gray lines represent the prior ensemble and the blue lines represent the posterior ensemble, red dots are the measurements.



Besides the data matching, the update of the model parameters ensemble must be analyzed in order to verify if the main characteristics of the prior ensemble are preserved, avoiding a poor uncertainty assessment and forecast prediction of the reservoir model. Two parameters that can be analyzed are the differences between the prior and posterior ensemble members (the model plausibility) and the changes in the standard deviations between the prior and posterior ensemble (uncertainty assessment). Figure 24 presents the distributions for the water-oil contact of the east sector (local scalar parameter) and the rock compressibility (global scalar parameter). The posterior distributions of water-oil contact (Figure 24a) for the restricted cases present larger variability in relation to the case without localization. This illustrates the importance of restricting the scalar parameters when it is possible, since in the cases without the restriction, the posterior distribution tends to ensemble collapse, as can be observed in all cases for the rock compressibility (Figure 24b).

Figure 24 - Distribution of prior and posterior water-oil contact of the east block and rock compressibility.

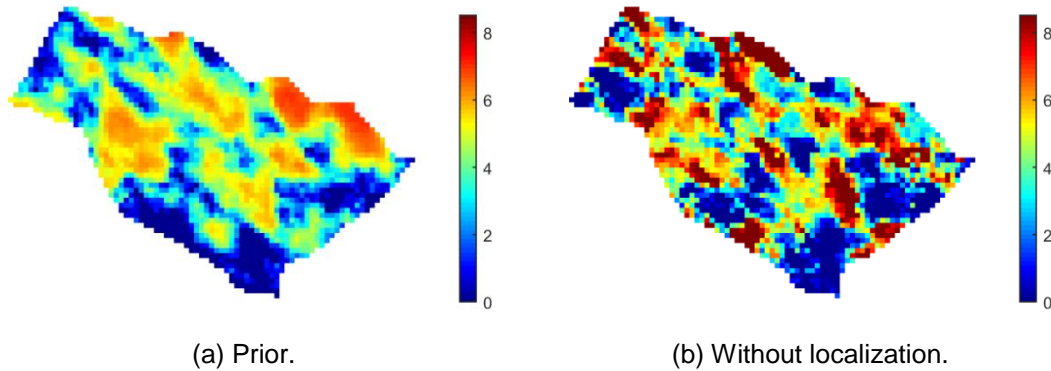


(a) Distribution for the water-oil contact of the east sector.

(b) Distribution for the rock compressibility.

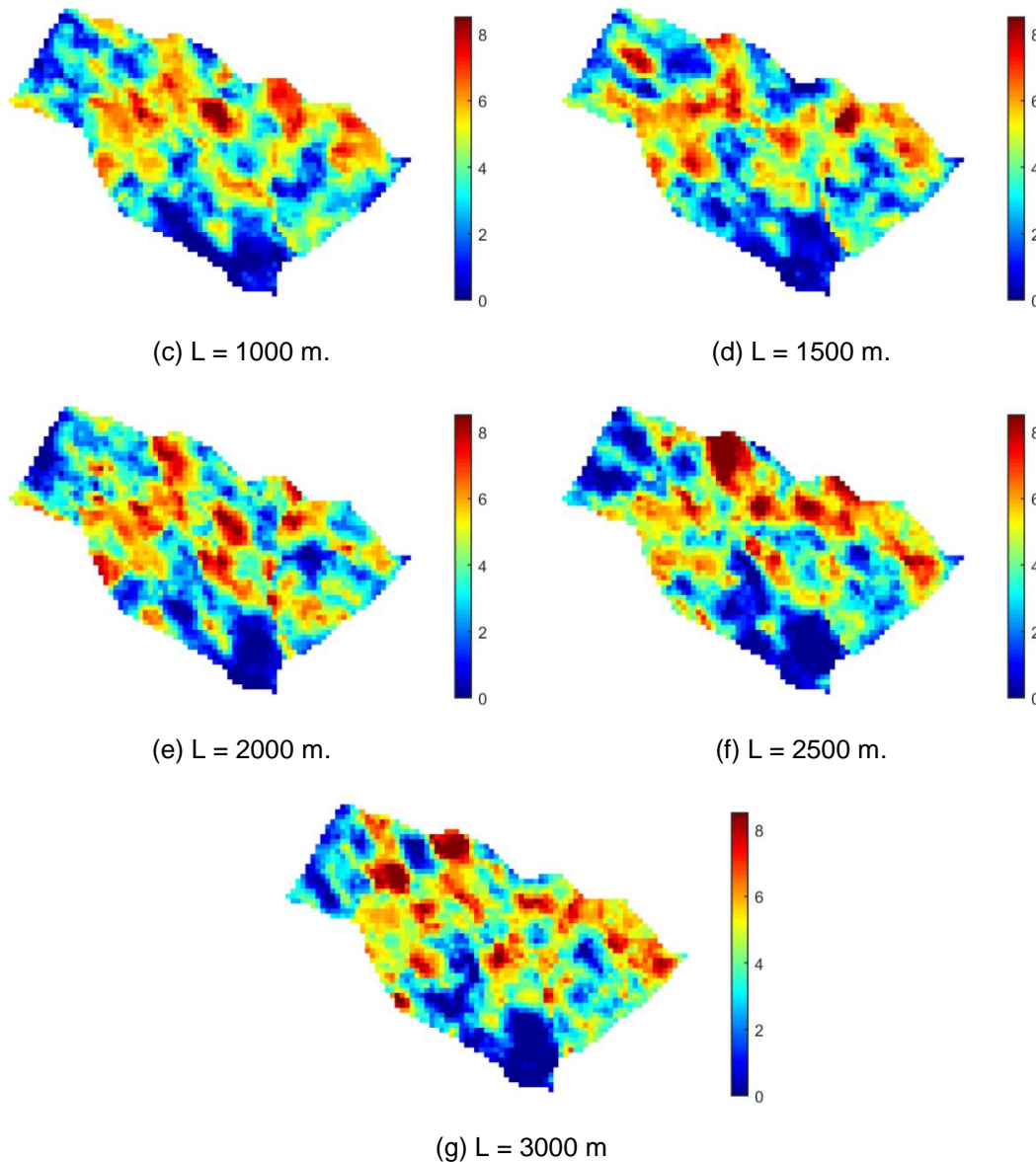
The \tilde{O}_{Nm} mean values in Table 2 show a relationship between the critical length and the mismatch of the prior and posterior ensemble. The cases presented similar values for the data mismatch objective function mean (except for $L = 1000$ m) but different values for the model mismatch objective function mean, showing the importance of the properly selection of the localization parameters. Figure 25 shows the log-permeability in i-direction ($\ln(k_i)$) for the first realization of the prior and posterior models, and it is possible to see how the localization is able to preserve the characteristics of the prior model. It is also possible to verify that the case without localization generates high roughness and extreme values in the updated model.

Figure 25 - First layer log-permeability field in i-direction of the first realization before and after the assimilation for different critical lengths.



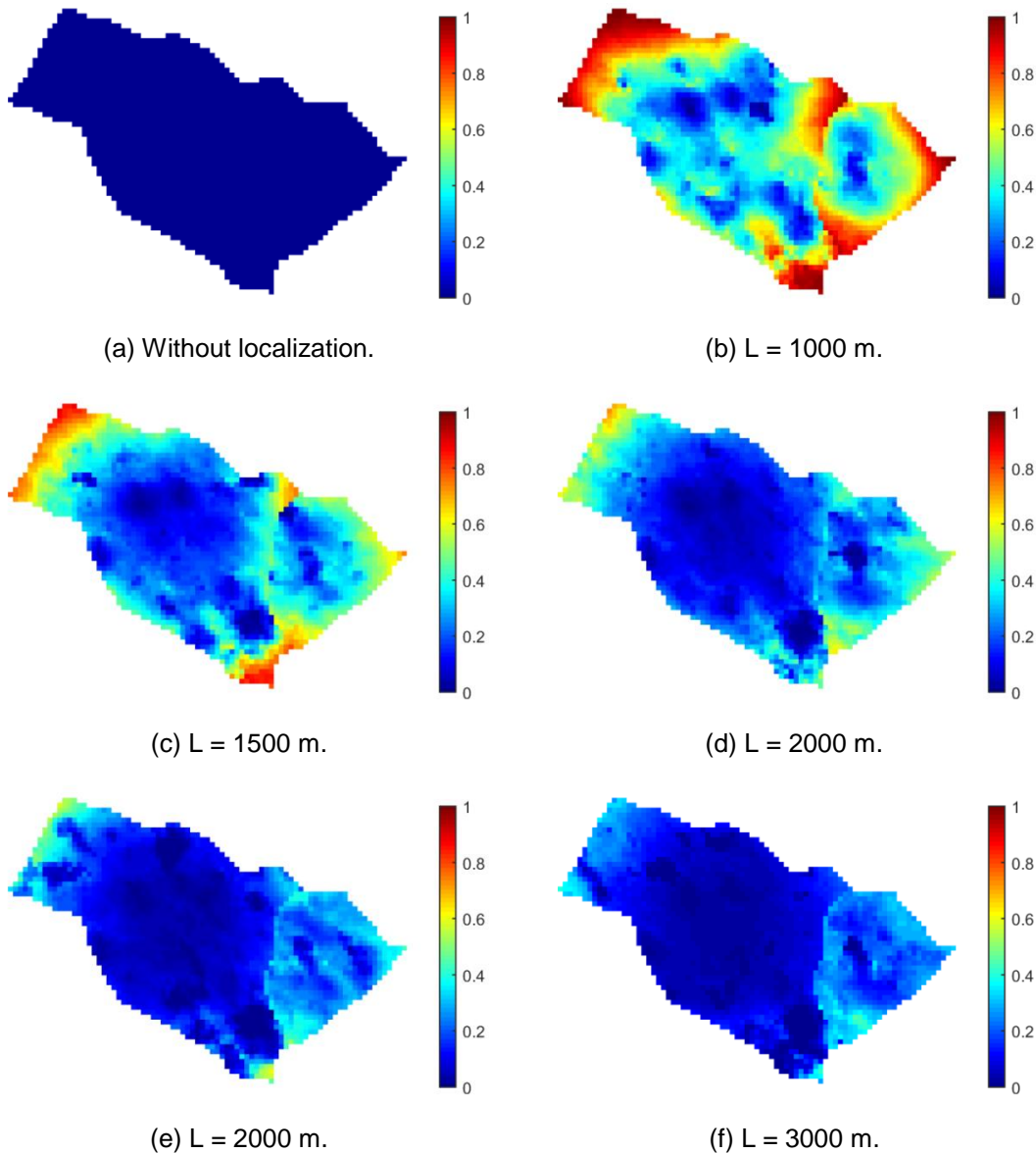
(a) Prior.

(b) Without localization.



An effective way to quantify the uncertainty reduction in field parameters after the update is through the normalized variance maps (relation between the posterior and prior variance of the model parameters) (SOARES; MASCHIO; SCHIOZER, 2018; EMERICK, 2018). Figure 26 shows the normalized variance of the first layer log-permeability in i -direction ($\ln(k_i)$). It is possible to verify the ensemble collapse in the case without localization, and a large uncertainty reduction as the critical length increases. It is also possible to observe a better uncertainty assessment in the east sector, probably an effect of the restriction imposed in the localization matrix, where the relation N_m/N_e is lower in the east sector than the west, providing a better posterior sampling of model parameters ensemble, since according to Evensen (2003). It is expected that a larger ensemble is needed to assimilate the whole model parameters (N_m -size) than only a local subset of them.

Figure 26 - Normalized variance of prior and posterior models of log-permeability in i-direction for different critical lengths.



3.5 Conclusions

This work performed an adaptive history matching with a distance-based localization method in a synthetic large-scale reservoir model. The main conclusions obtained are:

- The adaptive ES-MDA showed consistent results, presenting a considerable reduction of the data mismatch for all cases, making the history matching process easier since the number of iterations is estimated by the algorithm, which has the efficiency to continue the iteration process regardless of the choice of inflation factors.

- The results indicate that the localization does have influences in the process when an adaptive algorithm is applied, as can be seen when the lowest critical length in the study ($L = 1000$ m) resulted in a high number of iterations (that greatly increases the total computational time) to complete the algorithm, and in addition presenting higher values for the data-mismatch objective function (\bar{O}_{Nd} equal to 19.54 for $L = 1000$ m).
- The simple fact of restricting a scalar parameter when possible, showed an improvement in their posterior sampling, as observed when using localization in the water-oil contact of the east sector.
- Only data matching evaluation is not a sufficient parameter to analyze the quality of the matching, because, in this work, different critical lengths showed similar data matchings.
- An important analysis to be made is the quantification of the mismatch between the prior and posterior parameters, in order to preserve the characteristics of the prior ensemble. In this work, an approximation of the C_M matrix was able to estimate these mismatches, being possible to establish a direct relation between the model mismatches and the critical length used in localization.
- Localization techniques are fundamental in large-scale problems in order to prevent roughness and ensemble collapse, as can be seen in the posterior model of the case without localization.

3.6 Acknowledgments

The authors would like to thank the Polytechnic School of the University of São Paulo, CAPES (Coordination for the Improvement of Higher Education Personnel), FAPESP (São Paulo Research Foundation) and LASG (Laboratory of Petroleum Reservoir Simulation and Management) for supporting this research and study development, and CMG (Computer Modelling Group Ltd.) for providing the reservoir simulator licenses used in this study. The authors are grateful for the valuable feedback by the anonymous reviewers that made this paper easier to read.

CHAPTER 4 - CONCLUSIONS

In an adaptive ES-MDA, the total number of iterations and the inflation factors required to perform the methodology are automatically selected by the algorithm. When the ES-MDA is applied in a large-scale reservoir history matching problem, these parameters had unknown behavior as function of some input parameters, for example, localization and ensemble size. We decided to investigate these parameters applying the methodology in a large-scale reservoir simulation model. After the investigation, it is possible to point out some important conclusions.

In Chapter 2, it is possible to conclude that ensemble size does not have any influence on the number of iterations and inflation factors. In this point of view, ensemble size must be selected according to the balance between the uncertainty reduction and computational time required to run the ensemble (as already known for other iterative methods).

However, when localization was investigated in Chapter 3, we verified that a higher reduction of the measurements influence can modify the number of iterations, and beyond that, it presents worse matchings in comparison with a higher influence of the measurements. This fact highlights the importance of correct implement the localization, even more when adaptive methodologies are applied.

4.1 Future Research

The conclusion of the importance of the localization obtained in this work open the possibility of new studies to a broad area. One example is the necessity of evaluating the impact of the localization in carbonate reservoirs. Carbonate reservoirs require a high-resolution characterization and modeling with Dual-Porosity and Dual-Permeability simulation grids (MAUCEC et al.; 2016). In addition, carbonate reservoirs also have the necessity to model hydraulic connections and Super-k features (very thin layers with high porosity and permeability). This reinforces the necessity of developing a robust localization methodology, since the distance only cannot be enough to represent the influence between the parameter and data in high heterogeneity reservoirs. Confirming this point of view, Maucec et al. (2016) pointed out the need to investigate the effects of streamline-based localization in carbonate reservoirs as possible solution to overcome the difficulties related to the high heterogeneity.

Another thing that can be examined is the adaptive methodology itself (the way to automatically select the number of iterations and inflation factors). No best adaptive method emerged as the main methodology for history matching. Some previous works have proposed other adaptive methodologies, for example, ES-MDA-RLM (LE; EMERICK; REYNOLDS, 2016), ES-MDA-GEO (RAFIEE; REYNOLDS, 2017).

The ES-MDA-RLM method is fully automatic (inflation factors and number of iterations defined automatically) with an interesting Levenberg-Marquardt scheme, but in some previous tests that we performed in UNISIM-I-H, the algorithm did not converge as the required number of iterations being unfeasible. For this reason, we did not use the method in this dissertation. On the other hand, the ES-MDA-GEO has an interesting way of selecting the inflation factors, with proven improvements due his selection scheme (RAFIEE; REYNOLDS, 2017). However, the number of iterations in this method still need to be defined by the user. So, it is possible to conclude that the development of adaptive methodologies will become the main history matching researches goal.

REFERENCES

- AANONSEN, S.I.; NÆVDAL, G.; OLIVER, D.S.; REYNOLDS, A.C.; VALLÈS, B. The Ensemble Kalman Filter in Reservoir Engineering – a Review. **SPE Journal**, v. 14, n. 3, p. 393-412, 2009.
- AVANSI, G.D.; SCHIOZER, D.J. UNISIM-I: Synthetic Model for Reservoir Development and Management Applications. **International Journal of Modeling and Simulation for the Petroleum Industry**, v. 9, n. 1, p. 21-30, 2015.
- BRESLAVICH, I.D.; SARKISOV, G.G.; MARAKOVA, E.S. Experience of MDA Ensemble Smoother Practice for Volga-Ural Oilfield. In: SPE RUSSIAN PETROLEUM TECHNOLOGY CONFERENCE. **Proceedings...** Moscow, Russia, 16-18 October, 2017.
- BURGERS, G.; VAN LEEUWEN, P.J.; EVENSEN, G. Analysis Scheme in the Ensemble Kalman Filter. **Monthly Weather Review**, v. 126, n. 6, p. 1719-1724, 1998.
- CHEN, Y.; OLIVER, D.S. Ensemble Randomized Maximum Likelihood Method as an Iterative Ensemble Smoother. **Mathematical Geosciences**, v. 44, n. 1, p. 1-26, 2012.
- CHEN, Y.; OLIVER, D.S. Ensemble-Based Closed-Loop Optimization Applied to Brugge Field. **SPE Reservoir Evaluation & Engineering**, v. 13, n. 1, p. 56-71, 2010.
- CHEN, Y.; OLIVER, D.S. History Matching of the Norne Full-Field Model with an Iterative Ensemble Smoother. **SPE Reservoir Evaluation & Engineering**, v. 17, n. 2, p. 244-256, 2014.
- CHEN, Y.; OLIVER, D.S. Levenberg-Marquardt forms of the iterative ensemble smoother for efficient history matching and uncertainty quantification. **Computational Geosciences**, v. 17, p. 689-703, 2013.
- CHEN, Y.; OLIVER, D.S. Localization and regularization for iterative ensemble smoothers. **Computational Geosciences**, v. 21, n. 1, p. 13-30, 2016.
- COATS, K.H. Use and Misuse of Reservoir Simulation Models. **Journal of Petroleum Technology**, v. 21, n. 11, p. 1391-1398, 1969.
- EMERICK, A.A. Analysis of the performance of ensemble-based assimilation of production and seismic data. **Journal of Petroleum Science and Engineering**, v. 139, p. 219-239, 2016.
- EMERICK, A.A. Deterministic ensemble smoother with multiple data assimilation as an alternative for history-matching seismic data. **Computational Geosciences**, v. 22, n. 5, p. 1175-1185, 2018.
- EMERICK, A.A., REYNOLDS, A.C. Combining sensitivities and prior information for covariance localization in the ensemble Kalman filter for petroleum reservoir applications. **Computational Geosciences**, v. 15, n. 2, p. 251-269, 2011b.
- EMERICK, A.A., REYNOLDS, A.C. Ensemble Smoother with multiple data assimilation. **Computers & Geosciences**, v. 55, p. 3-15, 2013.

EMERICK, A.A., REYNOLDS, A.C. History Matching a Field Case using the Ensemble Kalman Filter with Covariance Localization. **SPE Reservoir Evaluation & Engineering**, v. 14, n. 4, p. 423-432, 2011a.

EVENSEN, G. Analysis of iterative ensemble smoother for solving inverse problems. **Computational Geosciences**, v. 22, n. 3, p. 885-908, 2018.

EVENSEN, G. **Data Assimilation: The Ensemble Kalman Filter**. Berlin: Springer-Verlag, 2007.

EVENSEN, G. Sampling strategies and square root analysis schemes for the EnKF. **Ocean Dynamics**, v. 54, p. 539-560, 2004.

EVENSEN, G. Sequential data assimilation with a nonlinear quasi-geostrophic model using Monte Carlo methods to forecast error statistics. **Journal of Geophysical Research**, v. 99, n. C5, p. 10143-10162, 1994.

EVENSEN, G. The Ensemble Kalman Filter: theoretical formulation and practical implementation. **Ocean Dynamics**, v. 53, p. 343-367, 2003.

FURRER, R.; BENGTSSON, T. Estimation of high-dimensional prior and posterior covariances matrices in Kalman filter variants. **Journal of Multivariate Analysis**, v. 98, n. 2, 227-255, 2007.

GASPAR, A.T.; SANTOS, A.A.; MASCHIO, C.; AVANSI, G.D.; FILHO, J.H.; SCHIOZER, D.J. Study Case for Exploitation Strategy Selection based on UNISIM-I Field, 2015. Available online: www.unisim.cepetro.unicamp.br/benchmarks/en/unisim-i/unisim-i-d

GASPARI G.; COHN, S.E. Construction of correlation functions in two and three dimensions. **Quarterly Journal of the Royal Meteorological Society**, v. 125, n. 554, p. 723-757, 1999.

GU, Y.; OLIVER, D.S. An Iterative Ensemble Kalman Filter for Multiphase Fluid Flow Data Assimilation. **SPE Journal**, v. 12, n. 4, p. 438-446, 2007.

HAUGEN, V.; NÆVDAL, G.; NATVIK, L.-J.; EVENSEN, G.; BERG, A.M.; FLORNES K.M. History Matching Using the Ensemble Kalman Filter on a North Sea Field Case. **SPE Journal**, v. 13, n. 4, p. 382-391, 2008.

HEIDARI, L.; GERVAIS, V.; RAVALEC, M.L.; WACKERNAGEL, H. History matching of petroleum reservoir models by the Ensemble Kalman Filter and parameterization methods. **Computers & Geosciences**, v. 55, p. 84-95, 2013.

IGLESIAS, M.A. Iterative regularization for ensemble data assimilation in reservoir models. **Computational Geosciences**, v. 19, n. 1, p. 177-212, 2015.

IGLESIAS, M.A.; DAWSON, C. The regularizing Levenberg-Marquardt scheme for history matching of petroleum reservoirs. **Computational Geosciences**, v. 13, n. 6, 1033-1053, 2013.

KALMAN, R.E. A New Approach to Linear Filtering and Prediction Problems. **Journal of Basic Engineering**, v. 82, n. 1, p. 35-45, 1960.

LE, D.H.; EMERICK, A.A.; REYNOLDS, A.C. An Adaptive Ensemble Smoother with Multiple Data Assimilation for Assisted History Matching. **SPE Journal**, v. 21, n. 6, p. 2195-2207, 2016.

MA, X.; HETZ, G.; WANG, X.; BI L.; STERN, D.; HODAN. A Robust Iterative Ensemble Smoother Method for Efficient History Matching and Uncertainty Quantification. In: SPE RESERVOIR SIMULATION CONFERENCE. **Proceedings...** Montgomery, Texas, USA, 20-22 February, 2017.

MASCHIO, C.; AVANSI, G.; SCHIOZER, D.; SANTOS, A. Study Case for History Matching and Uncertainties Reduction based on UNISIM-I Field, 2015. Available online: www.unisim.cepetro.unicamp.br/benchmarks/br/unisim-i/unisim-i-h

MAUCEC, M.; RAVANELLI, F.M.; LYNGRA, S.; ZHANG, S.J.; ALRAMADHAN, A.A.; ABDELHAMID, O.A.; AL-GARNI, S.A. Ensemble-Based Assisted History Matching with Rigorous Uncertainty Quantification applied to a Naturally Fractured Carbonate Reservoir. In: SPE ANNUAL TECHNICAL CONFERENCE & EXHIBITION. **Proceedings...** Dubai, UAE, 26-28 September, 2016.

MOROSOV, A.L.; SCHIOZER, D.J. Field-Development Process Revealing Uncertainty-Assessment Pitfalls. **SPE Reservoir Evaluation & Engineering**, v. 20, n. 3, p. 1-14, 2017.

NÆVDAL, G.; JOHNSEN, L.M.; AANONSEN, S.I., VEFRING, E.H. Reservoir Monitoring and Continuous Model Updating Using Ensemble Kalman Filter. In: SPE ANNUAL TECHNICAL CONFERENCE AND EXHIBITION. **Proceedings...** Denver, Colorado, USA, 5-8 October, 2003.

NÆVDAL, G.; MANNSETH, T.; VEFRING, E.H. Near-Well Reservoir Monitoring Though Ensemble Kalman Filter. In: SPE/DOE IMPROVED OIL RECOVERY SYMPOSIUM. **Proceedings...** Tulsa, Oklahoma, USA, 13-17 April, 2002.

OLIVER, D.S.; CHEN, Y. Recent progress on reservoir history matching: a review. **Computational Geosciences**, v. 15, n. 1, p. 185-221, 2011.

OLIVER, D.S.; REYNOLDS, A.C.; LIU N. **Inverse Theory for Petroleum Characterization and History Matching**. New York: Cambridge University Press, 2008.

RAFIEE, J.; REYNOLDS, A.C. Theoretical and efficient practical procedures for the generation of inflation factors for ES-MDA. **Inverse Problems**, v. 33, n. 11, p. 1-28, 2017.

RANAZZI, P.H.; SAMPAIO, M.A. Analysis of Ensemble Size influence on the Ensemble Smoother in the History Matching process (In Portuguese). In: RIO OIL & GAS EXPO AND CONFERENCE. **Proceedings...** Rio de Janeiro, Brazil, 24-27 September, 2018.

RANAZZI, P.H.; SAMPAIO, M.A. Influence of the Kalman Gain Localization in Adaptive Ensemble Smoother History Matching. **Journal of Petroleum Science and Engineering**, v. 179, p. 244-256, 2019.

RWECHUNGURA, R.; DADASHPOUR, M.; KLEPPE J. Advanced History Matching Techniques Reviewed. In: SPE MIDDLE EAST OIL AND GAS SHOW AND CONFERENCE. **Proceedings**... Manama, Bahrain, 25-28 September, 2011.

SANTOS, J.P.M. **Determinação de Metodologia de Ajuste Automatizado de Histórico**. 100 p. Thesis (Master of Science) – Faculdade de Engenharia Mecânica, Universidade de Campinas, Campinas, 2000.

SEILER, A.; EVENSEN, G.; SKJERVHEIM, J.-A.; HOVE, J.; VABØ, J.G. Advanced Reservoir Management Workflow Using an EnKF Based Assisted History Matching Method. In: SPE RESERVOIR SIMULATION SYMPOSIUM. **Proceedings**... the Woodlands, Texas, USA, 2-4 February, 2009.

SHUAI, Y.; WHITE, C.; SUN, T.; FENG, Y. A gathered EnKF for continuous reservoir model updating. **Journal of Petroleum Science and Engineering**, v. 139, p. 205-218, 2016.

SILVA, V.L.S.; EMERICK, A.A.; COUTO, P.; ALVES, J.L.D. History matching and production optimization under uncertainties – Application of closed-loop reservoir management. **Journal of Petroleum Science and Engineering**, v. 157, p. 860-874, 2017.

SKJERVHEIM, J.-A.; EVENSEN, G.; HOVE, J.; VABØ, J.G. An Ensemble Smoother for assisted History Matching. In: SPE RESERVOIR SIMULATION SYMPOSIUM. **Proceedings**... The Woodlands, Texas, USA, 21-23 February, 2011.

SOARES, R.V.; MASCHIO, C.; SCHIOZER, D.J. Applying a localization technique to Kalman Gain and assessing the influence on the variability of models in history matching. **Journal of Petroleum Science and Engineering**, v. 169, p. 110-125, 2018.

TARANTOLA, A. **Inverse Problem Theory and Methods for Model Parameter Estimation**. Philadelphia: SIAM, 2005.

THULIN, K.; LI, G.; AANONSEN, S.I.; REYNOLDS, A.C. Estimation of Initial Fluid Contacts by Assimilation of Production Data with EnKF. In: SPE ANNUAL TECHNICAL CONFERENCE AND EXHIBITION. **Proceedings**... Anaheim, California, USA, 11-14 November, 2007.

THULIN, K.; NÆVDAL, G.; SKAUG, H.J.; AANONSEN, S.I. Quantifying Monte Carlo Uncertainty in the Ensemble Kalman Filter. **SPE Journal**, v. 16, n. 01, p. 172-182, 2011.

VAN LEEUWEN, P.J.; EVENSEN, G. Data Assimilation and Inverse Methods in Terms of a Probabilistic Formulation. **Monthly Weather Review**, v. 124, p. 2898-2913, 1996.

WANG, Y.; LI, G.; REYNOLDS, A.C. Estimation of Depths of Fluid Contacts and Relative Permeability Curves by History Matching Using Iterative Ensemble-Kalman Smoothers. **SPE Journal**, v. 15, n. 2, p. 509-525, 2010.

WATANABE, S.; DATTA-GUPTA, A. Use of Phase Streamlines for Covariance Localization in Ensemble Kalman Filter for Three-Phase History Matching. **SPE Reservoir Evaluation & Engineering**, v. 15, n. 3, p. 273-289, 2012.

XU, Z.; CHENG, L.; WU, Y.; HUANG, P.J.; FANG, S.; HAO, J.; GAO Y. History Matching and Uncertainty Assessment by Using the Ensemble Kalman Filter. In:

OFFSHORE TECHNOLOGY CONFERENCE ASIA. **Proceedings...** Kuala Lumpur, Malaysia, 20-23 March, 2018.

ZAFARI, M.; REYNOLDS, A.C. Assessing the Uncertainty in Reservoir Description and Performance Predictions with the Ensemble Kalman Filter. In: SPE ANNUAL TECHNICAL CONFERENCE AND EXHIBITION. **Proceedings...** Dallas, Texas, USA, 9-12 October, 2005.

ZHANG, Y.; OLIVER, D.S. History Matching Using the Ensemble Kalman Filter with Multiscale Parameterization: A Field Case Study. **SPE Journal**, v. 16, n. 2, p. 307-317, 2011.